Title: Apoptosis in mesenchymal stromal cells induces *in vivo* recipient-mediated immunomodulation

Overline: Transplantation

Single sentence summary: Mesenchymal stromal cell apoptosis, induced *in vivo* by recipient cytotoxic cells, is required for immunosuppression and clinical responses

Authors: Antonio Galleu[1], Yanira Riffo-Vasquez[2], Cristina Trento[1], Cara Lomas[3,4], Luigi Dolcetti[1], Tik Shing Cheung[1], Malte von Bonin[5], Laura Barbieri[1], Krishma Halai[1], Sophie Ward[3,4], Ling Weng[1], Ronjon Chakraverty[3,4], Giovanna Lombardi[6], Fiona M. Watt[7], Kim Orchard[8], David I. Marks[9], Jane Apperley[10], Martin Bornhauser[1,5], Henning Walczak*[4], Clare Bennett*[3,4], and Francesco Dazzi[1,10]

* Contributed equally

Affiliations: [1]Regenerative Medicine, Division of Cancer Studies, King's College London, London SE5 9NU, UK. [2]Institute of Pharmaceutical Science, King's College London, London SE1 9NH, UK. [3]UCL Institute of Immunity and Transplantation, London NW3 2QG, UK. [4]UCL Cancer Institute, London WC1E 6DD, UK. [5]University Hospital Carl Gustav Carus, 01307 Dresden, Germany. [6]MRC Centre for Transplantation King's College London, London SE1 9RT, UK. [7]Centre for Regenerative Medicine, King's College London, London SE1 9RT, UK. [8]Southampton University Hospitals Trust, Southampton SO16 6YD, UK. [9]Haematology and Oncology Centre, Bristol BS2 8ED, UK. [10]Centre for Haematology, Imperial College London, London W12 0NN, UK.

Abstract

The immunosuppressive activity of mesenchymal stromal cells (MSC) is well documented. However, the therapeutic benefit is completely unpredictable, thus raising concerns about MSC efficacy. One of the affecting factors is the unresolved conundrum that, despite being immunosuppressive, MSC are undetectable following administration. Therefore, understanding the fate of infused MSC could help to predict clinical responses. Using a murine model of graft-versus-host disease (GvHD) we demonstrate that MSC are actively induced to undergo perforin-dependent apoptosis by recipient cytotoxic cells and that this process is essential to initiate MSC-induced immunosuppression. When examining patients with GvHD who received MSC we found a striking parallel, whereby only those with high cytotoxic activity against MSC responded to MSC infusion whereas those with low activity did not. Importantly, the need for recipient cytotoxic cell activity could be replaced by the infusion of apoptotic MSC generated *ex vivo*. After infusion, recipient phagocytes engulf apoptotic MSC and produce indoleamine 2,3-dioxygenase (IDO) that is ultimately necessary for effecting immunosuppression. Therefore, we propose the innovative concept that patients should be stratified for MSC treatment according to their ability to kill MSC or that all patients could be treated with *ex vivo* apoptotic MSC.

Introduction

Mesenchymal stromal cells (MSC) have received center stage attention because they exhibit potent immunosuppressive and anti-inflammatory activities (*1*) that have been extensively tested in several medical conditions, ranging from autoimmune diseases to the immunological complications of clinical transplantation (*2–5*). The extensive clinical use has been undeterred by the fact that the mechanisms underlying MSC therapeutic activity remain largely unresolved. MSC mediated immunosuppression is major histocompatibility complex (MHC)-independent, non antigen-specific (*1*), and targets virtually all immune cells by arresting cell cycle progression (*6–8*). Interference with aminoacid metabolism in the inflammatory microenvironment has been suggested as a crucial mechanism with indoleamine 2-3 dioxygenase (IDO) being one of the major candidates (*9, 10*), along with transforming growth factor-β1, hepatocyte growth factor (*11*), prostagladin E2 (*12*) and soluble human leukocyte antigen G (*13, 14*). TNF–α stimulated gene 6 protein (TSG-6) has been identified as a recent addition to the anti-inflammatory armamentarium of human MSC (*15*). However, there is consensus that the immunosuppressive activity does not solely rely on MSC but may involve the active engagement of other immunomodulatory cells, such as regulatory T cells (*16, 17*) and immunosuppressive macrophages (*18, 19*).

The imperfect knowledge of MSC immunobiology may well explain why the results of the clinical trials have often been controversial and why conclusive proof of efficacy has not yet been provided. Two major unresolved challenges undermine progress in the field. The first is that, only a proportion of patients, although affected by the same disease, responds to MSC infusions and this response cannot be predicted. The second is that, to be efficacious, MSC are not required to engraft. The vast majority of infused MSC resides transiently in the lungs before becoming undetectable within a few hours (*20*). Since our current knowledge cannot provide an explanation to this paradox (*6, 9, 10, 15*), a better understanding of the mechanisms underlying MSC therapeutic activity would be highly desirable to improve clinical efficacy and make therapeutic achievements more reproducible. We selected to address these challenges in graft-versus-host disease (GvHD) because there is proof of

principle that MSC are clinically efficacious (*4, 21*). By using a mouse model and clinical samples, we have tested the hypothesis that MSC undergo *in vivo* apoptosis following exposure to the GvHD environment.

Results

MSC undergo apoptosis in recipient GvHD animals.

We utilized a mouse model of GvHD in which lethally irradiated C57BL/6 male mice were transplanted on day 0 with bone marrow (BM), polyclonal purified CD4$^+$ T cells from female syngeneic donors and purified CD8$^+$ T cells transgenic for a T-cell receptor specific for the mouse male HY-antigen Uty (Matahari, Mh) as GvHD effectors (*22*) (Fig. S1A). The addition of CD4$^+$ T cells is necessary to facilitate the expansion of the CD8$^+$ T cells. In this model the expansion of the T cells effecting GvHD (CD8$^+$Vβ8.3$^+$) can be precisely enumerated and correlates with the clinical severity of the disease. Human MSC were injected 3 days after the transplant.

In order to explain the mechanism by which MSC are rapidly cleared after injection (*20, 23*) we tested the hypothesis that MSC undergo apoptosis.

In vivo MSC caspase activation was evaluated as a read-out of apoptosis. MSC were transfected with the pGL3-control vector for the expression of firefly luciferase (*Luc*+) (luc-MSC). Caspase activation was measured as luciferase activity using injection of DEVD-aminoluciferin. In this system, caspase 3 activation could be quantified on the basis of emitted light since DEVD is cleaved upon activation of caspase 3, leading to release of aminoluciferin which in turn can be metabolized by the firefly luciferase expressed in MSC. Luc-MSC were injected into recipients of BM transplant with CD8$^+$ Mh T cells (GvHD group) and one hour later caspase activity was measured *in vivo* as total luminescence signal (TLS). Two groups of control mice received MSC. One consisted of untreated males (naïve group) and the second was a group of mice which were irradiated and also received CD4$^+$ T cells and BM cells (BM group) without the transgenic CD8$^+$ T cells to reproduce the condition of MSC infusion in the absence of activated cytotoxic T cells (Fig. S1A). We observed

high caspase activity only in MSC injected into GvHD mice (Fig. 1, A and B). High signal could be detected from the lungs of all animals when the control D-luciferin (firefly luciferase substrate) was used (Fig. S1, B and C), thus confirming that luc-MSC can be tracked in the lungs also when caspase activity could not be detected.

The evidence that MSC undergo apoptosis after infusion prompted the question of whether they are still capable of suppressing antigen-driven T cell expansion. Therefore, we analyzed their immunosuppressive effect by enumerating CD8$^+$Vβ8.3$^+$ Mh T cells (GvHD effector cells) in MSC-treated or -untreated GvHD mice. MSC produced a substantial reduction in GvHD effector cell infiltration in both spleen and lungs (Fig. 1, C and D). These results indicate that, despite the presence of MSC apoptosis after infusion (Fig. 1, A and B), MSC immunosuppression still occurs. We can likely exclude the possibility that the observed immunosuppressive activity could be the consequence of the recipient inflammatory cytokines because in our xenogeneic combination murine inflammatory cytokines will not cross-react with the corresponding human receptors and will not activate immunosuppressive molecules in human MSC (*24–26*), whilst retaining the ability to expand murine effector cells mediating GvHD (*27*). Accordingly, human MSC were not able to inhibit concanavalin-A (ConA) induced proliferation of murine splenocytes (mSpl) unless pre-activated by human cytokines (Fig. S2, A, B and C). Furthermore, exposure of human MSC to murine inflammatory cytokines did not upregulate *IDO*, TNF-stimulated gene 6 protein (*TSG-6*) or prostaglandin-endoperoxide synthase-2 (*PTSG2*), considered major effectors of human MSC-mediated *in vitro* immunosuppression (Fig. S2 D).

In vivo MSC apoptosis depends on activated recipient GvHD effector cells
Our results show that MSC rapidly undergo apoptosis after infusion, providing an explanation for the rapid clearance of transplanted MSC in the recipient. The absence of *in vivo* MSC apoptosis in the control groups (naïve and BM mice) clearly demonstrates that MSC apoptosis is not the result of xenogeneic recognition of human MSC, because it is detected only in GvHD mice. When we enumerated GvHD effector cell infiltrate (CD8$^+$Vβ8.3$^+$) in the lungs of mice, where MSC apoptosis

occurs, we found that only the lungs of GvHD but not naïve and BM mice contained a large proportion of CD8$^+$Vβ8.3$^+$ cells (Fig. 2A), thus confirming the correlation between caspase activation in MSC and the presence of GvHD effector cells.

To test the hypothesis that GvHD effector cells were responsible for MSC apoptosis, MSC were cultivated with CD8$^+$ T cells purified from the lungs or spleens of GvHD (*in vivo* activated) or naïve Mh (*in vivo* resting) mice. Activated, but not resting, Mh CD8$^+$ T cells induced MSC apoptosis (Fig. 2B). Similar proportion of cytotoxicity against MSC could be elicited by naïve Mh CD8$^+$ T cells stimulated *in vitro* by CD3/CD28 beads (Fig. S3A).

The requirement of cytotoxic cells in the induction of MSC apoptosis and the consequent immunosuppression was evaluated using Mh/Perforin Knock-Out mice (Mh/Perf$^{-/-}$) as donors of defective cytotoxic GvHD effector cells (GvHDPerf$^{-/-}$ group). Luc-MSC were infused into GvHDPerf$^{-/-}$ or control GvHD mice which had received Mh CD8$^+$ T cells. Mice were imaged 1 hour later and caspase activation measured as described above. We observed much lower caspase activity in GvHDPerf$^{-/-}$ mice compared to GvHD controls (Fig. 2, C and D). High signal was detected in the lungs of all animals when the control D-luciferin was used (Fig. S3, B and C), thus confirming that luc-MSC were in the lungs also when caspase activity could not be detected. Importantly, the infiltration of GvHD effector cells in the spleen and lungs of mice receiving MSC was not reduced in GvHDPerf$^{-/-}$ receiving MSC (Fig. 2, E and F). We conclude that MSC apoptosis is indispensable for immunosuppression and requires functionally activated cytotoxic cells in the recipient.

Cytotoxic activity against MSC is associated with clinical response to MSC in GvHD patients
Based on these findings, we inferred that the presence of cytotoxic cells in the recipient could be predictive of MSC therapeutic activity. Sixteen patients, mean age 40.5 years (range: 10-69), with severe steroid resistant grade 3-4 GvHD received a total of 17 doses of MSC. Patient characteristics are summarized in Table S1.

Clinical responses to MSC were defined by an improvement of at least 50% in at least 1 organ affected by GvHD, as previously described (*4, 21, 28*). Five patients obtained a clinical response. Peripheral blood mononuclear cells (PBMC) were freshly collected within the 24 hours preceding the MSC infusion and tested directly for their ability to induce MSC apoptosis *ex vivo* in a 4-hour cytotoxic assay. One patient received two doses of MSC and the cytotoxic assay was performed before each dose independently. MSC were sourced from the same donor used for the infusion (*N*=8) or from a different donor (*N*=9). At the time of performing the assay and cytofluorimetric analysis the operator was blind to patients' clinical details. PBMC from healthy donors (*N*=5) were used as controls.

Overall, PBMC from GvHD patients and control PBMC exhibited similar cytotoxic activity against MSC (mean±SD were: 10.63±8.76% and 3.82±2.50%, respectively; p=.10). However, cytotoxicity between clinical responders and non-responders to MSC was markedly different, with the proportion of apoptotic MSC (annexin-V$^+$/7AAD$^-$) exhibiting a four-fold difference (Fig. 3, A and B). The discrimination threshold of apoptotic MSC between responders and non-responders calculated using the receiver-operating characteristic curve revealed that a 14.85% cut-off was predictive of clinical response with the highest sensitivity and specificity. Cytotoxicity did not vary amongst MSC preparations, because when we tested patients' PBMC against the MSC used for the infusion as compared to another preparation obtained from an unrelated donor, no difference in apoptosis induction could be detected (Fig. S4A). To further confirm the irrelevance of the specific MSC preparation, we evaluated the susceptibility of MSC sourced from different unrelated donors to undergo apoptosis after exposure to 4 different mixed lymphocyte reaction (MLR) combinations. The proportion of apoptotic MSC was similar amongst the different MSC preparations when the same MLR was tested. Conversely, the cytotoxic activity against the same MSC varied amongst different MLR (Fig. S4, B).

Finally, we ruled out the possibility that different proportions of CD8$^+$ and CD56$^+$ cells could account for the differing cytotoxic activity because the average frequency in the PBMC of responders and

non-responders was similar (Fig. S4, C and D). Therefore, we conclude that the presence of activated cytotoxic cells in the recipient is predictive of MSC therapeutic activity.

MSC apoptosis induced by cytotoxic cells is the result of a bystander effect

To define the mechanisms that drive apoptosis in MSC, we used *in-vitro*-activated PBMC from healthy donors as effector cells. We found that activated but not resting PBMC induced extensive early apoptosis (annexin-V$^+$/7AAD$^-$) in MSC (Fig. 4A), which peaked at 4 hours and shifted towards late apoptosis (annexin-V$^+$/7AAD$^+$) by 24 hours (Fig. S5A). In accord with our *in vivo* observations (Fig. 1, A and B), only activated PBMC induced caspase activation in MSC with a peak at 90 minutes (Video S1, S2 and S3), and this was completely abrogated by the pan-caspase inhibitor Z-VAD-FMK (Fig. 4B, Fig. S5B and Video S4).

In order to identify the cells inducing apoptosis in MSC, we performed selective enrichment and depletion experiments amongst activated PBMC. We found that CD56$^+$ natural killer (NK) and CD8$^+$ T cell populations were the only cells responsible for initiating MSC apoptosis (Fig. 4, C and D). To characterize the mechanisms mediating MSC apoptosis induced by activated cytotoxic cells, we studied potential factors involved in caspase 3 activation. Inhibition of either Granzyme B (GrB) or perforin completely abolished the ability of activated PBMC to kill MSC (Fig. 4E) and activate caspase 3 (Fig. S5C, Video S5 and S6). We also observed reduced PBMC-mediated cytotoxicity when CD95 ligand (CD95L, also known as FasL or APO-1L) was neutralized (Fig. 4F), but not when Tumor Necrosis Factor-α (TNF-α) or TNF-related apoptosis-inducing ligand (TRAIL) were inhibited, even in the presence of very high concentrations of their respective inhibitors (Fig. S5D).

We then interrogated the nature of the MSC-cytotoxic cell interaction. We observed that apoptosis was not affected by the presence of anti-HLA class I- or anti-HLA class II neutralizing antibodies. Consistently, the cytotoxic activity of activated PBMC against autologous or allogeneic MSC did not differ (Fig. 4G). However, although PBMC required physical contact with MSC to induce apoptosis (Fig. 4H), blocking immunological synapse formation by inhibiting the polarization of microtubule

organizing center (*29*) had no effect (Fig. 4I). These results demonstrate that MSC killing by activated cytotoxic cells is a bystander effect that does not involve the immunological synapse.

MSC apoptosis does not interfere with the recognition of the specific target of cytotoxic cells

Having determined that the MSC apoptosis induced by cytotoxic cells is MHC-independent and not antigen-specific, we asked whether MSC could exert their immunosuppressive effects by competing with and antagonizing antigen-specific recognition. NY-ESO1-specific human CD8$^+$ T cell clone (4D8) or IL2-activated polyclonal human CD56$^+$ purified NK cells were used as effector cells against NY-ESO-1 peptide pulsed T2 or K562 target cells, respectively. T2 cells are deficient in a peptide transporter for antigen processing (TAP) and therefore can only present exogenously pulsed peptides (*30*). K562 is a leukaemia cell line selectively sensitive to NK cytotoxicity (*31*). Two different sets of experiments were performed. In the first set, 4D8 or NK cells were tested against fixed numbers of putative (*susceptible*) target cells in the presence of escalating numbers of MSC used as a *cold* target. The alternative condition consisted of escalating the numbers of the putative specific target cells – now used as *cold* targets – in the presence of a fixed number of MSC then considered as the *susceptible* target. MSC did not compete with antigen-specific T cell cytotoxicity, since the killing of peptide-pulsed T2 cells was not affected by the presence of MSC (Fig. 5A). The same results were obtained using NK cells (Fig. 5B). In contrast, the presence of the putative target cells markedly reduced MSC killing in a dose dependent manner in both systems (Fig. 5, C and D). Our data show that MSC killing does not interfere with the primary recognition of the cognate antigen.

Apoptotic MSC are immunosuppressive in a Th2-type inflammation model

Our data imply that, since MSC killing does not interfere with the primary recognition of the cognate antigen, induction of apoptosis must be prominently involved in the immunosuppressive activity. Accordingly, in the GvHD model described above, MSC apoptosis produced by recipient cytotoxic cells is required for immunosuppression. Therefore, we asked whether this causative relationship remains valid in a different disease model associated with non-cytotoxic Th2-type inflammation. We

selected the model of ovalbumin (OVA)-induced allergic airway inflammation (32) summarized in Fig. S6A. Although cytotoxic immune cells have been implicated as contributing to the induction of this condition (33, 34), CD8$^+$ and NK1.1$^+$ cells infiltrating bronchoalveolar lavage (BAL) and lung tissues were less than 2% one hour after the last OVA challenge, when MSC were infused (Fig. S6, B, C, D and E). To confirm the absence of MSC killing, mice received luc-MSC to assess caspase activation after infusion and imaged one hour later. No caspase activation was detected in any of the mice (Fig. 6, A and B). High signal could be detected in all animals receiving control D-luciferin (Fig. S6, F and G).

The therapeutic activity, assessed by quantitating the eosinophil infiltration in the BAL showed no difference between MSC-treated and untreated mice (Fig. 6C). Together, these results indicate that also in this model MSC immunosuppression relies on the presence of recipient cytotoxic cells that mediate MSC apoptosis. Therefore, we decided to test whether MSC, made apoptotic *in vitro* by exposure to FasL and granzyme B (apoMSC), could bypass the need of cytotoxic cells in the recipient and ameliorate eosinophil infiltration. When apoMSC were administered to recipient mice we observed that the eosinophil infiltration in BAL was much reduced (Fig. 6D).

Apoptotic MSC infused in GvHD are immunosuppressive and induce IDO production in recipient phagocytes

We subsequently investigated whether apoMSC could be immunosuppressive also in the GvHD model. ApoMSC were administered either intravenously (i.v.). or intraperitoneally (i.p.). and the infiltration of CD8$^+$Vβ8.3$^+$ Mh T cells was assessed and compared to untreated GvHD mice. ApoMSC produced a substantial reduction in GvHD effector cell infiltration in both spleen and lungs, but this could only be observed in those mice treated with ApoMSC infused i.p. (Fig. 7, A, B, C and D).

It has been reported that the injection of irradiated thymocytes into animals results in their phagocytosis by recipient macrophages and induction of IDO (35). We therefore tested whether

apoMSC followed the same destiny by eliciting *in vivo* efferocytosis by recipient phagocytes and inducing IDO production. For this purpose, labelled apoMSC were traced in recipient phagocytes after injection. Following i.p. administration, apoMSC were largely identified inside CD11b$^+$ (Fig. 7, E) and CD11c$^+$ (Fig. 7, F) phagocytes in the peritoneal draining lymph nodes (*36*) but absent when searched for in the lungs and spleen. When the i.v. route was used, amongst the several phagocytic populations investigated (*37*) CD11b^{high}CD11c^{int}, CD11b^{high}CD11c$^-$ and CD11b$^-$CD11c$^+$ were detected as engulfing apoMSC in lungs (Fig. 7, G, H and I, respectively). The analysis of IDO expression in the phagocytes engulfing ApoMSC both in the i.v. and i.p. groups revealed that only the phagocytes in the i.p. group were able to increase IDO expression in comparison with their counterparts in untreated GvHD mice (Fig. 7, J and K). These findings strongly suggest that the immunosuppressive effect of apoMSC involve recipient phagocytes and IDO as crucial effector mechanisms.

Recipient-derived IDO-producing phagocytes are indispensable for MSC immunosuppression in GvHD

To directly test the importance of recipient-derived phagocytes and recipient-produced IDO in MSC immunosuppressive activity, we depleted phagocytes and inhibited IDO activity in GvHD mice before MSC treatment and evaluated the effect of live MSC on the expansion of GvHD effectors. To deplete phagocytes, liposome clodronate was given to mice 72 hours before MSC injection. The treatment substantially impaired the ability of MSC to suppress Mh T cell infiltration (Fig. 8, A and B). Finally, animals were given the IDO inhibitor 1-methyl-D-tryptophan (1-DMT) (38) before MSC injection. Also in this case, the beneficial effect of MSC on Mh T cell infiltration was much reduced in mice receiving 1-DMT compared to controls (Fig. 8, C and D). We therefore conclude that the immunosuppressive effect of MSC requires the presence of recipient phagocytic cells or IDO production.

Discussion

This study sheds light on the controversial topic of MSC therapeutics by identifying a crucial mechanism that potentially explains several unresolved issues in the field. The first striking piece of information provides the resolution to the paradox that MSC are therapeutically efficacious despite the lack of engraftment (39–41). We demonstrate that MSC undergo extensive caspase activation and apoptosis after infusion in the presence of cytotoxic cells, and that this is a requirement for their immunosuppressive function. Although other recipient-dependent reactions have been described as mediating MSC lysis *in vitro* (42) and MSC clearance *in vivo* (40, 41, 43, 44) our study has shown the instrumental role of *in vivo* MSC apoptosis in delivering immunosuppression after infusion. Furthermore, although several studies *(38, 45–47)* have reported the ability of apoptotic cells to modulate immune responses, here we provide evidence that *in vivo* naturally occurring cell death drives immunosuppression.

MSC apoptosis requires and is effected by cytotoxic granules contained in recipient cytotoxic cells that also mediate GvHD in recipient mice. Importantly, the cytotoxic activity against MSC can also be detected in the PBMC of GvHD patients and it is predictive of clinical responses. Patients displaying high cytotoxicity respond to MSC, whilst those with low or absent cytotoxic activity do not improve following MSC infusion. Therefore, the ability of the recipient to generate apoptotic MSC appears to be a requirement for the therapeutic efficacy and could be used as a potential biomarker to stratify patients for MSC infusions. However, the limited number of patients analyzed prompts further validation in a clinical study. Moreover, characterizing the phenotype of the cytotoxic cells mediating MSC apoptosis in patients, can provide important information for the development of a routine biomarker assay.

MSC recognition by cytotoxic cells is not antigen-specific as neither requires HLA engagement nor results from an alloreactive rejection, thus supporting the current practice of using third-party MSC. MSC must be in physical contact with the activated cytotoxic cells to undergo apoptosis, although

immunological synapse is not required. This supports a bystander role for the cytotoxic granules released by the activated cytotoxic cell. Accordingly, it has been described that lytic granule secretion precedes the formation of cytotoxic T lymphocyte/target cell synapse *(29)*. Furthermore, such a non-specific mechanism can mediate tissue damage in the context of HIV replication *(48) or* atherosclerosis *(49)* whereby activated CD4$^+$ or natural killer T (NKT) cells have been implicated in the progression of HIV infection or the atherosclerotic disease, respectively. In these studies, bystander cells are not of mesenchymal origin, thus raising the interesting question, that we have not addressed here, of whether nonspecific induction of apoptosis and subsequent immunosuppression is selective for MSC.

Our data suggest an approach to MSC therapeutics that highlights the key role of MSC recipient to orchestrate and determine MSC effector functions. Not only are cytotoxic cells in the recipient required to initiate apoptosis in infused MSC, but also phagocytes which, by engulfing apoptotic MSC and producing IDO, ultimately deliver MSC immunosuppressive activity. Similar mechanisms have been described to explain how apoptotic cells of different lineages, generated *in vitro*, induce immune modulation in GvHD *(45–47)* and macrophage IDO production in other systemic autoimmune diseases *(38)*. This is also consistent with the described ability of MSC to stimulate recipient immune tolerance networks, like regulatory T cells and macrophages *(18, 19)*.

The depletion of recipient macrophages or the inhibition of IDO activity impairs also the therapeutic activity of live MSC, thereby linking *in vivo* MSC apoptosis with immunosuppression. It is unlikely that any particular phagocyte population (macrophages or dendritic cells) is selectively involved in engulfing apoMSC because they similarly display such an activity *in vivo*. However, since clodronate exhibits a preferential depleting activity on macrophages compared to dendritic cells, our data suggest macrophages to play a more important role.

One of the impacts of our study is that, although MSC remain the necessary starting point for therapeutic immunosuppression, patient-derived cells play a crucial role in delivering such an immunosuppression. Therefore, the efforts aimed at identifying the most clinically effective MSC subpopulation as well as the potency assays to validate such a selection may prove futile. A further proof supporting this concept is that the administration of *ex-vivo* generated apoMSC can circumvent the requirement for cytotoxic cells in a Th2 inflammatory model and that apoMSC can be effective at suppressing the expansion/infiltration of the GvHD effector cells. Interestingly, apoMSC were mostly effective in the GvHD model only when administered i.p. Despite being phagocytosed, apoMSC injected i.v. did not induce IDO production, thus suggesting that the site at which MSC apoptosis occurs may influence the immunosuppressive function, perhaps by engaging with a subpopulation of phagocytes. Therefore, a more thorough characterization of the administration modality is required before testing apoMSC in the clinical setting.

A final question is whether a cytokine-dependent 'licensing' *(25, 50)*, co-exists with the generation of apoptotic MSC. Although our data indicate that cytokine-licensing is not required for the therapeutic activity, we cannot exclude that, before undergoing apoptosis, MSC directly inhibit inflammatory reactions through the conventional pathways. Furthermore, caspase activation in MSC may trigger cell-death independent pathways that stimulate the synthesis of immunomodulatory molecules independently of the generation of signals for phagocytosis *(51)*. Consistent with this, it has been shown that MSC activate caspase-dependent IL-1 signaling that enhances secretion of immunomodulatory molecules *(52)*.

Our study constitutes a paradigm shift in MSC therapeutics whereby their apoptotic demise is a key step in the effector mechanism of immunosuppression exerted by MSC. A further impact of our discovery is that the principle underpinning this mechanism could be used as a biomarker to predict clinical responses to MSC and therefore stratify GvHD patients for MSC treatment. We therefore believe that the next generation of clinical trials should shift the focus from choosing the best MSC

population to choosing the patients most likely to respond. Furthermore, the intriguing possibility that apoMSC may be effective in patients refractory to MSC, paves the way to new avenues in the clinical manufacturing of MSC.

Materials and Methods

Study Design

This study aimed to verify whether MSC undergo apoptosis after infusion and to test the role played by MSC apoptosis in the initiation of recipient-derived tolerogenic immune response.

A mouse model of GvHD, in which the disease is mediated by the expansion and activation of Mh CD8$^+$ T cells in the recipient, was chosen for three important reasons: it recapitulates a minor mismatch between donor and recipient; T cells effecting GvHD can be precisely enumerated; there is proof-of-principle that MSC are effective in treating GvHD. Furthermore, human MSC were used in order to avoid the confounding effects of recipient cytokines on MSC immune-modulating function *(10, 50)*. In this system, murine inflammatory cytokines will not cross-react with the corresponding human receptors and will not activate immunosuppressive molecules in human MSC *(24–26)*, whilst retaining the ability to expand murine effector cells mediating GvHD. Depletion of phagocytes and inhibition of IDO production were conceived as loss of function experiments to assess the requirement of these factors in the delivery of MSC apoptosis-dependent immunosuppression.

A mouse model of ovalbumin (OVA)-induced allergic airway inflammation was used to assess whether the causative relationship between cytotoxic cells and MSC apoptosis in the delivery of MSC immunosuppression is valid in a disease associated with Th2-type inflammation.

All animal procedures were carried out in compliance with the UK Home Office Animals (Scientific Procedures) Act of 1986.

In all experiments, animals were randomly allocated to control or experimental groups. No blinding approach was adopted. No statistical method was used to predetermine sample size, which was estimated only on previous experience with assay sensitivity and the different animal models. Unless otherwise specified, three independent experimental replicates were performed.

To demonstrate that the presence of cytotoxic cells against MSC in GvHD patients could be predictive of MSC therapeutic activity, samples from GvHD patients were collected and tested for their ability to induce MSC apoptosis in a cytotoxic assay within 24 hours before MSC infusion. At the time of performing the assay and cytofluorimetric analysis, the operator was blind to patients' clinical details. All patients were affected by steroid-resistant GvHD and received MSC for compassionate use. PBMC from healthy donors were used as controls. All samples were collected after informed consent was obtained in accordance with the local ethics committee requirements. Primary data are located in table S2.

Mice and disease models

Acute GvHD was induced as previously described *(22)*. Briefly, after lethal irradiation (11 Gy), recipient C57BL/6 male mice were transplanted i.v. with 1×10^6 purified $CD8^+$ T cells from female Mh mice together with 5×10^6 unfractionated BM and 2×10^6 purified $CD4^+$ T cells from female C57BL/6 wild-type donors. The control group received BM and purified $CD4^+$ T cells only.

For the depletion of all phagocytes mice received 1 mg liposome clodronate (ClodronateLiposomes.com) i.v. 72 hours before MSC infusion *(35)*. Recipient IDO activity was inhibited by using 1-DMT treatment (Sigma-Aldrich Company Ltd) (2mg/ml) in the drinking water starting from 6 days prior to MSC injection until animals were sacrificed *(38)*.

C57BL/6-Prf1tm1Sdz/J (Perforin$^{-/-}$) mice were purchased from Jackson labs, bred with Matahari Rag2$^{-/-}$ mice and the resulting offspring intercrossed for 2 generations to obtain Mh Rag2$^{-/-}$.Perf KO F3 mice.

OVA-induced airway inflammation was induced as previously described *(32)*. Briefly, female Balb/C mice (Harlan Laboratories) were injected intraperitoneally with 30 µg of chicken egg albumin (OVA type V) (Sigma-Aldrich Company Ltd) on day 0 and 7. Controls received vehicle (aluminum hydroxide) only. On day 14, 15 and 16 animals were challenged with an aerosolized solution of OVA (3%) administered with De Vilibiss Ultraneb 90 for 25 minutes. MSC or ApoMSC were injected 1 hour after the last challenge. After additional 18 hours, mice were terminally anaesthetized, a cannula inserted into the exposed trachea and three aliquots of sterile saline were injected into the lungs to obtain BAL fluid. The total number of cells in the lavage fluid was counted.

MSC preparations

Clinical grade BM-derived human MSC were generated from BM aspirates collected from the iliac crest of healthy donors. The cells were plated at a density of 10-25 million/636 cm^2. After 3 days at 37 °C and 5% CO_2 non-adherent cells were discarded. When cell confluence of 90-100% was achieved, cells were detached with Trypsin-EDTA and reseeded at a density of 5000 cells/cm^2. MSC from different donors were used at passage 2 for all *in vivo* experiments, whilst they were used by passage 8 for the *in vitro* experiments. In the latter case, we did not observe any difference in terms of apoptosis susceptibility between different passages. In each experiments, MSC were derived from a single expansion and not pooled.

Patients

Between November 2012 and July 2016, 16 patients affected by steroid-resistant GvHD were treated with MSC according to Regulation (EC) No 1394/2007. All patients received GvHD prophylaxis. Of the 16 patients included in the study, 13 developed GvHD following hematopoietic stem cell transplantation, and the remaining 3 after Donor Lymphocyte Infusion (DLI). 12 patients were affected by acute GvHD, 3 by late onset acute GvHD and 1 by chronic GvHD. The diagnosis of GvHD was made on histological criteria and GvHD staged according to standard criteria *(53, 54)*. Patient characteristics are summarized in Table S1. Samples were collected within 24 hours before MSC injection.

Please see Supplementary Materials for full experimental procedures.

Statistics

Results were expressed as mean±SD. The unpaired Student *t* test was performed to compare 2 mean values. One-way ANOVA and Tukey's Multiple Comparison test was used to compare 3 or more mean values. Probability of null hypothesis less than 5% (p<.05, two-sided) was considered statistically significant.

Supplementary Materials

Supplemental Experimental Procedures

Figure S1. MSC can be traced in the lungs of mice after infusion

Figure S2. Human MSC immunosuppression is not 'licensed' by murine cytokines

Figure S3. MSC apoptosis is activated by cytotoxic cells in a non-antigen-specific manner

Figure S4. Cytotoxicity against MSC varies amongst PBMC donor but is independent on the percentage of CD8$^+$ or CD56$^+$ in GvHD patients

Figure S5. MSC killing is mediated by caspase 3 and effected by GrB and perforin

Figure S6. Infused MSC can be imaged in the lungs of mice with Th2-type lung inflammation

Table S1. Clinical features of GvHD patients

Table S2. Primary data

Video S1. Living cell imaging of FRET-MSC plated alone

Video S2. Living cell imaging of FRET-MSC plated with PHA-aPBMC

Video S3. Living cell imaging of FRET-MSC plated with resting PBMC

Video S4. Living cell imaging of FRET-MSC plated with PHA-aPBMC in the presence of the pan-caspase inhibitor Z-VAD-FMK

Video S5. Living cell imaging of FRET-MSC plated with PHA-aPBMC in the presence of the GrB inhibitor Z-AAD-CMK

Video S6. Living cell imaging of FRET-MSC plated with PHA-aPBMC in the presence of the perforin inhibitor EGTA

References and Notes

1. M. Krampera, S. Glennie, J. Dyson, D. Scott, R. Laylor, E. Simpson, F. Dazzi, Bone marrow mesenchymal stem cells inhibit the response of naive and memory antigen-specific T cells to their cognate peptide, *Blood* **101**, 3722–3729 (2003).

2. R. Ciccocioppo, M. E. Bernardo, A. Sgarella, R. Maccario, M. A. Avanzini, C. Ubezio, A. Minelli, C. Alvisi, A. Vanoli, F. Calliada, P. Dionigi, C. Perotti, F. Locatelli, G. R. Corazza, Autologous bone marrow-derived mesenchymal stromal cells in the treatment of fistulising Crohn's disease, *Gut* **60**, 788–798 (2011).

3. F. Dazzi, M. Krampera, Mesenchymal stem cells and autoimmune diseases, *Best Pr. Res Clin Haematol* **24**, 49–57 (2011).

4. F. von Dalowski, M. Kramer, M. Wermke, R. Wehner, C. Rollig, N. Alakel, F. Stolzel, S. Parmentier, K. Sockel, M. Krech, M. Schmitz, U. Platzbecker, J. Schetelig, M. Bornhauser, M. von Bonin, Mesenchymal Stromal Cells for Treatment of Acute Steroid-Refractory Graft Versus Host Disease: Clinical Responses and Long-Term Outcome, *Stem Cells* **34**, 357–366 (2016).

5. J. Tan, W. Wu, X. Xu, L. Liao, F. Zheng, S. Messinger, X. Sun, J. Chen, S. Yang, J. Cai, X. Gao, A. Pileggi, C. Ricordi, Induction therapy with autologous mesenchymal stem cells in living-related kidney transplants: a randomized controlled trial, *JAMA* **307**, 1169–1177 (2012).

6. S. Glennie, I. Soeiro, P. J. Dyson, E. W. Lam, F. Dazzi, Bone marrow mesenchymal stem cells induce division arrest anergy of activated T cells, *Blood* **105**, 2821–2827 (2005).

7. R. Ramasamy, H. Fazekasova, E. W. Lam, I. Soeiro, G. Lombardi, F. Dazzi, Mesenchymal stem cells inhibit dendritic cell differentiation and function by preventing entry into the cell cycle, *Transplantation* **83**, 71–76 (2007).

8. R. Ramasamy, C. K. Tong, H. F. Seow, S. Vidyadaran, F. Dazzi, The immunosuppressive effects of human bone marrow-derived mesenchymal stem cells target T cell proliferation but not its effector function, *Cell Immunol* **251**, 131–136 (2008).

9. R. Meisel, A. Zibert, M. Laryea, U. Gobel, W. Daubener, D. Dilloo, Human bone marrow stromal cells inhibit allogeneic T-cell responses by indoleamine 2,3-dioxygenase-mediated tryptophan degradation, *Blood* **103**, 4619–4621 (2004).

10. J. Su, X. Chen, Y. Huang, W. Li, J. Li, K. Cao, G. Cao, L. Zhang, F. Li, A. I. Roberts, H. Kang, P. Yu, G. Ren, W. Ji, Y. Wang, Y. Shi, Phylogenetic distinction of iNOS and IDO function in mesenchymal stem cell-mediated immunosuppression in mammalian species, *Cell Death Differ* **21**, 388–396 (2014).

11. M. Di Nicola, C. Carlo-Stella, M. Magni, M. Milanesi, P. D. Longoni, P. Matteucci, S. Grisanti, A. M. Gianni, Human bone marrow stromal cells suppress T-lymphocyte proliferation induced by cellular or nonspecific mitogenic stimuli, *Blood* **99**, 3838–3843 (2002).

12. S. Aggarwal, M. F. Pittenger, Human mesenchymal stem cells modulate allogeneic immune cell responses, *Blood* **105**, 1815–1822 (2005).

13. F. Morandi, L. Raffaghello, G. Bianchi, F. Meloni, A. Salis, E. Millo, S. Ferrone, V. Barnaba, V. Pistoia, Immunogenicity of human mesenchymal stem cells in HLA-class I-restricted T-cell responses against viral or tumor-associated antigens, *Stem Cells* **26**, 1275–1287 (2008).

14. Z. Selmani, A. Naji, I. Zidi, B. Favier, E. Gaiffe, L. Obert, C. Borg, P. Saas, P. Tiberghien, N. Rouas-Freiss, E. D. Carosella, F. Deschaseaux, Human leukocyte antigen-G5 secretion by human mesenchymal stem cells is required to suppress T lymphocyte and natural killer function and to induce CD4+CD25highFOXP3+ regulatory T cells, *Stem Cells* **26**, 212–222 (2008).

15. H. Choi, R. H. Lee, N. Bazhanov, J. Y. Oh, D. J. Prockop, Anti-inflammatory protein TSG-6 secreted by activated MSCs attenuates zymosan-induced mouse peritonitis by decreasing TLR2/NF-kappaB signaling in resident macrophages, *Blood* **118**, 330–338 (2011).

16. C. Prevosto, M. Zancolli, P. Canevali, M. R. Zocchi, A. Poggi, Generation of CD4+ or CD8+ regulatory T cells upon mesenchymal stem cell-lymphocyte interaction, *Haematologica* **92**, 881–888 (2007).

17. K. English, J. M. Ryan, L. Tobin, M. J. Murphy, F. P. Barry, B. P. Mahon, Cell contact, prostaglandin E(2) and transforming growth factor beta 1 play non-redundant roles in human mesenchymal stem cell induction of CD4+CD25(High) forkhead box P3+ regulatory T cells, *Clin Exp Immunol* **156**, 149–160 (2009).

18. S. M. Melief, E. Schrama, M. H. Brugman, M. M. Tiemessen, M. J. Hoogduijn, W. E. Fibbe, H. Roelofs, Multipotent stromal cells induce human regulatory T cells through a novel pathway

involving skewing of monocytes toward anti-inflammatory macrophages, *Stem Cells* **31**, 1980–1991 (2013).

19. K. Nemeth, A. Leelahavanichkul, P. S. Yuen, B. Mayer, A. Parmelee, K. Doi, P. G. Robey, K. Leelahavanichkul, B. H. Koller, J. M. Brown, X. Hu, I. Jelinek, R. A. Star, E. Mezey, Bone marrow stromal cells attenuate sepsis via prostaglandin E(2)-dependent reprogramming of host macrophages to increase their interleukin-10 production, *Nat Med* **15**, 42–49 (2009).

20. R. H. Lee, A. A. Pulin, M. J. Seo, D. J. Kota, J. Ylostalo, B. L. Larson, L. Semprun-Prieto, P. Delafontaine, D. J. Prockop, Intravenous hMSCs improve myocardial infarction in mice because cells embolized in lung are activated to secrete the anti-inflammatory protein TSG-6, *Cell Stem Cell* **5**, 54–63 (2009).

21. I. B. Resnick, C. Barkats, M. Y. Shapira, P. Stepensky, A. I. Bloom, A. Shimoni, D. Mankuta, N. Varda-Bloom, L. Rheingold, M. Yeshurun, B. Bielorai, A. Toren, T. Zuckerman, A. Nagler, R. Or, Treatment of severe steroid resistant acute GVHD with mesenchymal stromal cells (MSC), *Am J Blood Res* **3**, 225–238 (2013).

22. T. Toubai, I. Tawara, Y. Sun, C. Liu, E. Nieves, R. Evers, T. Friedman, R. Korngold, P. Reddy, Induction of acute GVHD by sex-mismatched H-Y antigens in the absence of functional radiosensitive host hematopoietic-derived antigen-presenting cells, *Blood* **119**, 3844–3853 (2012).

23. J. A. Ankrum, J. F. Ong, J. M. Karp, Mesenchymal stem cells: immune evasive, not immune privileged, *Nat. Biotechnol.* **32**, 252–260 (2014).

24. M. Krampera, L. Cosmi, R. Angeli, A. Pasini, F. Liotta, A. Andreini, V. Santarlasci, B. Mazzinghi, G. Pizzolo, F. Vinante, P. Romagnani, E. Maggi, S. Romagnani, F. Annunziato, Role for interferon-gamma in the immunomodulatory activity of human bone marrow mesenchymal stem cells, *Stem Cells* **24**, 386–398 (2006).

25. G. Ren, L. Zhang, X. Zhao, G. Xu, Y. Zhang, A. I. Roberts, R. C. Zhao, Y. Shi, Mesenchymal stem cell-mediated immunosuppression occurs via concerted action of chemokines and nitric oxide, *Cell Stem Cell* **2**, 141–150 (2008).

26. R. S. Waterman, S. L. Tomchuck, S. L. Henkle, A. M. Betancourt, A new mesenchymal stem cell (MSC) paradigm: polarization into a pro-inflammatory MSC1 or an Immunosuppressive MSC2 phenotype, *PLoS One* **5**, e10088 (2010).

27. J. Fu, D. Wang, Y. Yu, J. Heinrichs, Y. Wu, S. Schutt, K. Kaosaard, C. Liu, K. Haarberg, D. Bastian, D. G. McDonald, C. Anasetti, X. Z. Yu, T-bet is critical for the development of acute graft-versus-host disease through controlling T cell differentiation and function, *J. Immunol.* **194**, 388–397 (2015).

28. M. von Bonin, A. Kiani, U. Platzbecker, J. Schetelig, K. Holig, U. Oelschlagel, C. Thiede, G. Ehninger, M. Bornhauser, Third-party mesenchymal stem cells as part of the management of graft-failure after haploidentical stem cell transplantation, *Leuk Res* **33**, e215-7 (2009).

29. F. Bertrand, S. Muller, K. H. Roh, C. Laurent, L. Dupre, S. Valitutti, An initial and rapid step of lytic granule secretion precedes microtubule organizing center polarization at the cytotoxic T lymphocyte/target cell synapse, *Proc. Natl. Acad. Sci. U. S. A.* **110**, 6073–6078 (2013).

30. N. A. Hosken, M. J. Bevan, Defective presentation of endogenous antigen by a cell line expressing class I molecules., *Science* **248**, 367–70 (1990).

31. B. B. Lozzio, C. B. Lozzio, Properties and usefulness of the original K-562 human myelogenous leukemia cell line., *Leuk. Res.* **3**, 363–70 (1979).

32. Y. Riffo-Vasquez, A. R. Coates, C. P. Page, D. Spina, Mycobacterium tuberculosis chaperonin 60.1 inhibits leukocyte diapedesis in a murine model of allergic lung inflammation, *Am J Respir Cell Mol Biol* **47**, 245–252 (2012).

33. E. Hamelmann, A. Oshiba, J. Paluh, K. Bradley, J. Loader, T. A. Potter, G. L. Larsen, E. W. Gelfand, Requirement for CD8+ T cells in the development of airway hyperresponsiveness in a marine model of airway sensitization., *J. Exp. Med.* **183**, 1719–29 (1996).

34. M. Korsgren, C. G. Persson, F. Sundler, T. Bjerke, T. Hansson, B. J. Chambers, S. Hong, L. Van Kaer, H. G. Ljunggren, O. Korsgren, Natural killer cells determine development of allergen-induced eosinophilic airway inflammation in mice., *J. Exp. Med.* **189**, 553–62 (1999).

35. T. L. McGaha, Y. Chen, B. Ravishankar, N. van Rooijen, M. C. Karlsson, Marginal zone macrophages suppress innate and adaptive immunity to apoptotic cells in the spleen, *Blood* **117**, 5403–5412 (2011).

36. C. P. Parungo, D. I. Soybel, Y. L. Colson, S.-W. Kim, S. Ohnishi, A. M. DeGrand, R. G. Laurence, E. G. Soltesz, F. Y. Chen, L. H. Cohn, M. G. Bawendi, J. V Frangioni, Lymphatic drainage of the peritoneal space: a pattern dependent on bowel lymphatics., *Ann. Surg. Oncol.* **14**, 286–98 (2007).

37. M. Guilliams, I. De Kleer, S. Henri, S. Post, L. Vanhoutte, S. De Prijck, K. Deswarte, B. Malissen, H. Hammad, B. N. Lambrecht, Alveolar macrophages develop from fetal monocytes that differentiate into long-lived cells in the first week of life via GM-CSF, *J. Exp. Med.* **210**, 1977–1992 (2013).

38. B. Ravishankar, H. Liu, R. Shinde, P. Chandler, B. Baban, M. Tanaka, D. H. Munn, A. L. Mellor, M. C. Karlsson, T. L. McGaha, Tolerance to apoptotic cells is regulated by indoleamine 2,3-dioxygenase, *Proc. Natl. Acad. Sci. U. S. A.* **109**, 3909–3914 (2012).

39. L. von Bahr, I. Batsis, G. Moll, M. Hagg, A. Szakos, B. Sundberg, M. Uzunel, O. Ringden, K. Le Blanc, Analysis of tissues following mesenchymal stromal cell therapy in humans indicates limited long-term engraftment and no ectopic tissue formation, *Stem Cells* **30**, 1575–1578 (2012).

40. N. Eliopoulos, J. Stagg, L. Lejeune, S. Pommey, J. Galipeau, Allogeneic marrow stromal cells are immune rejected by MHC class I- and class II-mismatched recipient mice, *Blood* **106**, 4057–4065 (2005).

41. A. J. Nauta, G. Westerhuis, A. B. Kruisselbrink, E. G. Lurvink, R. Willemze, W. E. Fibbe, Donor-derived mesenchymal stem cells are immunogenic in an allogeneic host and stimulate donor graft rejection in a nonmyeloablative setting, *Blood* **108**, 2114–2120 (2006).

42. G. M. Spaggiari, A. Capobianco, S. Becchetti, M. C. Mingari, L. Moretta, Mesenchymal stem cell-natural killer cell interactions: evidence that activated NK cells are capable of killing MSCs, whereas MSCs can inhibit IL-2-induced NK-cell proliferation, *Blood* **107**, 1484–1490 (2006).

43. G. Moll, I. Rasmusson-Duprez, L. von Bahr, A. M. Connolly-Andersen, G. Elgue, L. Funke, O. A. Hamad, H. Lonnies, P. U. Magnusson, J. Sanchez, Y. Teramura, K. Nilsson-Ekdahl, O.

Ringden, O. Korsgren, B. Nilsson, K. Le Blanc, Are therapeutic human mesenchymal stromal cells compatible with human blood?, *Stem Cells* **30**, 1565–1574 (2012).

44. Y. Li, F. Lin, Mesenchymal stem cells are injured by complement after their contact with serum, *Blood* **120**, 3436–3443 (2012).

45. K. Mizrahi, I. Yaniv, S. Ash, J. Stein, N. Askenasy, Apoptotic signaling through Fas and TNF receptors ameliorates GVHD in mobilized peripheral blood grafts., *Bone Marrow Transplant.* **49**, 640–8 (2014).

46. A. E. Morelli, A. T. Larregina, Concise Review: Mechanisms Behind Apoptotic Cell-Based Therapies Against Transplant Rejection and Graft versus Host Disease., *Stem Cells* **34**, 1142–50 (2016).

47. M. Florek, E. I. Sega, D. B. Leveson-Gower, J. Baker, A. M. S. Müller, D. Schneidawind, E. Meyer, R. S. Negrin, Autologous apoptotic cells preceding transplantation enhance survival in lethal murine graft-versus-host models., *Blood* **124**, 1832–42 (2014).

48. J. Couturier, A. T. Hutchison, M. A. Medina, C. Gingaras, P. Urvil, X. Yu, C. Nguyen, P. Mahale, L. Lin, C. A. Kozinetz, J. E. Schmitz, J. T. Kimata, T. C. Savidge, D. E. Lewis, HIV replication in conjunction with granzyme B production by CCR5+ memory CD4 T cells: Implications for bystander cell and tissue pathologies, *Virology* **462**–**463**, 175–188 (2014).

49. Y. Li, P. Kanellakis, H. Hosseini, A. Cao, V. Deswaerte, P. Tipping, B. H. Toh, A. Bobik, T. Kyaw, A CD1d-dependent lipid antagonist to NKT cells ameliorates atherosclerosis in ApoE-/- mice by reducing lesion necrosis and inflammation, *Cardiovasc Res* **109**, 305–317 (2016).

50. M. Duijvestein, M. E. Wildenberg, M. M. Welling, S. Hennink, I. Molendijk, V. L. van Zuylen, T. Bosse, A. C. Vos, E. S. de Jonge-Muller, H. Roelofs, L. van der Weerd, H. W. Verspaget, W. E. Fibbe, A. A. te Velde, G. R. van den Brink, D. W. Hommes, Pretreatment with interferon-gamma enhances the therapeutic activity of mesenchymal stromal cells in animal models of colitis, *Stem Cells* **29**, 1549–1558 (2011).

51. D. Wallach, T. B. Kang, S. H. Yang, A. Kovalenko, The in vivo significance of necroptosis: Lessons from exploration of caspase-8 function, *Cytokine Growth Factor Rev* (2013), doi:10.1016/j.cytogfr.2013.12.001.

52. T. J. Bartosh, J. H. Ylostalo, N. Bazhanov, J. Kuhlman, D. J. Prockop, Dynamic compaction of human mesenchymal stem/precursor cells into spheres self-activates caspase-dependent IL1 signaling to enhance secretion of modulators of inflammation and immunity (PGE2, TSG6, and STC1), *Stem Cells* **31**, 2443–2456 (2013).

53. D. Przepiorka, D. Weisdorf, P. Martin, H. G. Klingemann, P. Beatty, J. Hows, E. D. Thomas, 1994 Consensus Conference on Acute GVHD Grading, *Bone Marrow Transpl.* **15**, 825–828 (1995).

54. A. H. Filipovich, D. Weisdorf, S. Pavletic, G. Socie, J. R. Wingard, S. J. Lee, P. Martin, J. Chien, D. Przepiorka, D. Couriel, E. W. Cowen, P. Dinndorf, A. Farrell, R. Hartzman, J. Henslee-Downey, D. Jacobsohn, G. McDonald, B. Mittleman, J. D. Rizzo, M. Robinson, M. Schubert, K. Schultz, H. Shulman, M. Turner, G. Vogelsang, M. E. Flowers, National Institutes of Health consensus development project on criteria for clinical trials in chronic graft-versus-host disease: I. Diagnosis and staging working group report, *Biol. Blood Marrow Transplant.* **11**, 945–956 (2005).

55. A. Valujskikh, O. Lantz, S. Celli, P. Matzinger, P. S. Heeger, Cross-primed CD8(+) T cells mediate graft rejection via a distinct effector pathway, *Nat Immunol* **3**, 844–851 (2002).

56. J.-L. Chen, A. J. Morgan, G. Stewart-Jones, D. Shepherd, G. Bossi, L. Wooldridge, S. L. Hutchinson, A. K. Sewell, G. M. Griffiths, P. A. van der Merwe, E. Y. Jones, A. Galione, V. Cerundolo, Ca2+ release from the endoplasmic reticulum of NY-ESO-1-specific T cells is modulated by the affinity of TCR and by the use of the CD8 coreceptor., *J. Immunol.* **184**, 1829–39 (2010).

57. L. He, X. Wu, F. Meylan, D. P. Olson, J. Simone, D. Hewgill, R. Siegel, P. E. Lipsky, Monitoring caspase activity in living cells using fluorescent proteins and flow cytometry, *Am J Pathol* **164**, 1901–1913 (2004).

Author Contributions: Conceptualization: A.G, H.W and F.D. Methodology: A.G., F.D, C.B, Y.R.V and R.C. Formal. Analysis: A.G and L.D. Investigation: A.G., Y.R.V., C.T., C.L., L.B., S.W., K.H., T.S.C. and L.W. Resources: F.D., K.O., D.I. M., J.A., M. V. B. and M. B. Visualization: A.G. and L.D. Writing - Original Draft: A.G. and F.D. Writing – Review & Editing: A.G., C.B., G.L., F. M. W., H.W. and F.D. Funding acquisition: F.D. Supervision: F.D.

Competing interests: The authors declare no competing financial interests.

Data and materials availability: Reasonable requests for additional data or materials will be fulfilled under appropriate agreements.

Figure captions

Figure 1. MSC undergo *in vivo* apoptosis after infusion without affecting immunosuppression. A: luc-MSC were injected i.v. into naïve, BM and GvHD mice 3 days after transplantation. All animals were then injected i.p. with DEVD-aminoluciferin and imaged 1 hour later. *N*: total of 6 (1 to 3 mice per group), grouped from 3 independent experiments. In each experiment, a different MSC expansion was used. White lines separate multiple photographs assembled in the final image. **B**: Total luminescence signal (TLS) was measured from the images of mice in Fig. 1A and shown as mean±SD. **C, D**: Percentage of GvHD effector cells (CD8$^+$V$_\beta$8.3$^+$) calculated in the lymphocyte gate (defined by the physical characteristics of the cells) in the spleen (**C**) and lungs (**D**) of GvHD mice (black circles) and GvHD mice treated with MSC (black squares), 4 days after MSC injection. *N*: 15 (GvHD) and 13 (GvHD+MSC) mice, grouped from 4 independent

experiments; mean±SD are shown. Statistics in B: one-way ANOVA, with Tukey's Multiple Comparison Test. **: p<.01, ***: p<.001, ns: not significant. In C and D: unpaired t-test. **: p<.01.

Figure 2. MSC apoptosis is important for immunosuppression and requires functionally activated cytotoxic cells in the recipient. A: The percentage of CD8$^+$Vβ8.3$^+$ cells in lung cell suspensions from naïve C57BL/6 male, BM or GvHD mice was analyzed in the lymphocyte population; mean±SD are shown. *N*: 12 (GvHD), 3 (BM) and (3 (naïve) mice, grouped from 3 independent experiments. **B:** CD8$^+$ cells were sorted from the lungs and spleens of naïve female Mh (grey bars) or GvHD mice (not treated with MSC) (white bars) 7 days after the transplant and tested for their ability to induce MSC apoptosis *in vitro*. The results show annexin-V$^+$/7-AAD$^-$ MSC (mean±SD) in 3 independent experiments (*N*=10 per group), black bar represents the value of apoptosis in MSC cultured alone used as control (*N*: 3) **C**: luc-MSC were infused in three independent experiments in GvHD (*N*=7) and GvHDPerf$^{-/-}$ (*N*=7) mice 3 days after transplantation. 1 hour later mice were injected with DEVD-aminoluciferin and imaged. White lines separate multiple photographs assembled in the final image. **D**: Total luminescence signal (TLS) was obtained from Fig. 2C and expressed as mean±SD. **E, F**: The percentage of effector GvHD cells (CD8$^+$V$_\beta$8.3$^+$) in the lymphocyte population was measured in the spleen (**E**) and lungs (**F**) of untreated GvHDPerf$^{-/-}$ (*N*=16) and GvHDPerf$^{-/-}$ (*N*=17) mice treated with MSC (mean±SD of 4 independent experiments). Statistics in A and B: one-way ANOVA, with Tukey's Multiple Comparison Test. *: p<.05; ***: p<.001. In D, E and F: unpaired t-test. ***: p<.001. ns: not significant.

Figure 3. Cytotoxic activity against MSC predicts clinical responses to MSC in GvHD patients. A, B: PBMC obtained from healthy controls (HC) or patients with GvHD receiving MSC in the following 24 hours were incubated in 24-well plates with MSC at a 20:1 PBMC:MSC ratio for 4 hours. Apoptosis was measured in MSC assessing the percentage of annexin-V$^+$/7-AAD$^-$ cells by flow-cytometry. (**A**) Representative plots for HC, clinical responders (R) and non-responders (NR). The panels on the left show the background apoptosis of MSC alone used in the corresponding cytotoxic assay (**B**) Apoptosis was compared among HC (circles, *N*=5), R (triangles; *N*=5) and NR (squares;

N=12). Statistics: one-way ANOVA and Tukey's Multiple Comparison test. ***: p<.0001. ns: not significant.

Figure 4. MSC apoptosis is mediated by activated CD8$^+$ and CD56$^+$ cytotoxic cells and is the result of a bystander effect. A: PBMC from healthy donors (each independent experiment used a different PBMC donor) were activated using phytohemagglutinin (PHA) (PHA-aPBMC) or MLR (MLR-aPBMC). Resting (grey bars), PHA-aPBMC (black bars) or MLR-aPBMC (dashed bars) were incubated with MSC at the indicated ratios and MSC apoptosis (annexin-V$^+$/7-AAD$^-$) calculated after 4 hours. ND: Not done. **B**: Apoptosis in MSC cultivated with MLR-aPBMC in the presence or absence of the pan-caspase inhibitor Z-VAD-FMK (10 µM) or the corresponding concentration of its vehicle (DMSO). **C, D**: Apoptosis in MSC cultivated with MLR-aPBMC used as unfractionated or positively selected for CD11b$^+$, CD4$^+$, CD8$^+$ or CD56$^+$ cells (**C**) or depleted of CD56$^+$, CD8$^+$ or both (**D**). **E**: Apoptosis in MSC cultivated with MLR-aPBMC in the presence or absence of the GrB inhibitor Z-AAD-CMK (300 µM) or the perforin inhibitor ethylene glycol-bis(2aminoethylether)-N,N,N',N'-tetraacetic acid (EGTA) (4 mM). **F**: Apoptosis in MSC cultivated with PHA-aPBMC in the presence or absence of neutralizing concentrations (10 µg/ml and 100 µg/ml) of FAS-L mAb anti-CD178. **G**: Apoptosis in MSC after culture with autologous (black bars) or allogeneic (grey bars) PHA-aPBMC in the presence or absence of neutralizing doses of anti-HLA-A-B-C or anti-HLA-DR antibodies. The white bar shows spontaneous apoptosis in MSC plated alone. **H**: Apoptosis in MSC cultivated with MLR-aPBMC in direct contact or in a transwell. **I**: Apoptosis in MSC cultivated with PHA-aPBMC in the presence or absence of escalating doses (10 to 75 µM) of PKCζ-PS. In **B-I** the PBMC:MSC ratio was 20:1. Results represent the mean±SD of 3 or 6 (H) independent experiments. Statistics: one-way ANOVA, with Tukey's Multiple Comparison Test. *: p<0.5. **: p<.01. ***: p<.001. ns: not significant.

Figure 5. MSC do not compete with cytotoxic cell recognition of the cognate target. A: apoptosis in T2-cell after culture with 4D8 cells at a 20:1 4D8:T2 ratio. Where indicated increasing concentrations of MSC (used as *cold* target) were added. Apoptotic T2 cells were identified as annexin-V$^+$/7-AAD$^+$ cells. **B**: apoptosis in K562 cultured with NK cells (20:1 NK:K562 ratio). Where

indicated increasing concentrations of MSC (used a *cold* target) were added. **C**: apoptosis in MSC cultured with 4D8 cells (20:1 4D8:MSC ratio). Where indicated increasing concentrations of T2 cells (used as *cold* target) were added. **D**: apoptosis in MSC cultured with NK cells at a 20:1 NK:MSC ratio. Where indicated, increasing dilutions of K562 (used as *cold* target) were added. In all experiments apoptosis of MSC, T2 or K562 cells was assessed after 4 hours of co-culture by flow cytometry. Results represent the mean±SD of 3 independent experiments. Statistics in **A**, **B**, **C** and **D**: one-way ANOVA and Tukey's Multiple comparison test. *: p<.05.

Figure 6. Apoptotic MSC exert *in vivo* immunosuppression in a Th2-type inflammation model in the absence of cytotoxic cells. A: luc-MSC were injected into naïve (*N*=3) and OVA+MSC (*N*=6) mice one hour after the last challenge. One hour later, mice received DEVD-aminoluciferin and were imaged in 3 independent experiments. White lines separate multiple photographs assembled in the final image. **B**: Total luminescence signal (TLS) was measured from Fig. 6A (mean±SD). **C**: Eighteen hours after MSC infusion, eosinophil infiltration was assessed in the BAL of naïve (*N*=3), naïve infused with MSC (*N*=3), OVA (*N*=6) and OVA+MSC (*N*=6) mice in two independent experiments and mean±SD are shown. **D**: eosinophil infiltration (mean±SD) evaluated in BAL cytospin preparations from OVA-sensitized mice treated with ApoMSC. Groups were: OVA without ApoMSC (*N*=6), OVA treated with 1x10^6 ApoMSC (*N*=7); and naïve mice receiving 1x10^6 (*N*=2) ApoMSC. Results represent the mean±SD of 3 independent experiments. Statistics in **B**: unpaired t-test. ns: not significant. Statistics in **C and D**: one-way ANOVA and Tukey's Multiple comparison test. *: p<.05. ns: not significant.

Figure 7. ApoMSC exert immunosuppressive activity in GvHD and elicit IDO in engulfing recipient phagocytes. A-D: The percentage of GvHD effector cells was assessed in the lymphocyte gate in spleen (A, C) and lungs (B, D) of GvHD mice (black circles) and GvHD mice treated with ApoMSC (black squares). ApoMSC were infused i.p. (GvHD mice *N*=10, GvHD+ApoMSC mice *N*=8) (A, B), or i.v. (GvHD mice *N*=9, GvHD+ApoMSC mice *N*=7) (C, D). Results represent the mean±SD of 3 independent experiments. Statistics: unpaired t-test. *: p<.05; **: p<.01. ns: not significant. **E-K**: MSC were labelled using CellTrace™ Violet and subjected to

apoptosis induction using GrB/FAS-L (5 µg/ml and 10 µg/ml, respectively). ApoMSC were injected i.p. (E, F and J) or i.v. (G, H, I and K) into GvHD mice 3 days after the transplant. After 2 hours, animals were sacrificed and mesenteric lymph nodes (LN) (E, F and J) or lungs (G, H, I and K) were harvested. Cells engulfing ApoMSC were identified as Violet$^+$ cells within the CD11b$^+$ (E), CD11c$^+$ (F), CD11b^{high}CD11c^{int} (G), CD11c$^+$CD11b$^-$ (H) and CD11b^{high}CD11c$^-$ (I) subpopulations. The corresponding subpopulations were gated in GvHD mice which had not received violet-labelled ApoMSC and used as controls. **J** and **K**: IDO expression was assessed in CD11c$^+$ and CD11b$^+$ (J) or CD11b^{high}CD11c^{int}, CD11c$^+$CD11b$^-$ and CD11b^{high}CD11c$^-$ (K) cells positive for CellTrace^{TM} Violet (engulfing apoMSC) and compared with the corresponding populations in GvHD mice that had not received ApoMSC. Data are representative of similar results obtained from three mice in 2 independent experiments.

Figure 8. Recipient phagocytes and IDO production are required for MSC immunosuppressive activity in GvHD. **A, B:** GvHD mice were treated with liposomal clodronate 10 minutes after the transplant. Where indicated, MSC were infused 3 days later. The percentage of GvHD effector cells (CD8$^+$Vβ8.3$^+$) were calculated in the lymphocyte gate in spleen (A) or lungs (B) after 4 additional days. Mean±SD was obtained grouping three independent experiments with *N*: 12 (GvHD) and 10 (GvHD+MSC) mice per group. **C, D:** GvHD effector cell infiltration was studied in spleen (C) and lungs (D) of GvHD mice treated with the IDO-inhibitor 1-DMT. In the treated mice, MSC were infused 3 days after the transplant (*N*=11). Controls consisted of GvHD mice which did not receive MSC (*N*=9). Percentage of CD8$^+$Vβ8.3$^+$ cells refers to the lymphocyte population. Results refers to the mean±SD of 3 independent experiments. Statistics: unpaired t-test. *: p<.05; **: p<.01. ns: not significant.

Supplementary Materials

Apoptosis in mesenchymal stromal cells is required to initiate *in vivo* recipient-mediated immunomodulation

Antonio Galleu, Yanira Riffo-Vasquez, Cristina Trento, Cara Lomas, Luigi Dolcetti, Tik Shing Cheung, Malte von Bonin, Laura Barbieri, Krishma Halai, Sophie Ward, Ling Weng, Ronjon Chakraverty, Giovanna Lombardi, Fiona M. Watt, Kim Orchard, David I. Marks, Jane Apperley, Martin Bornhauser, Henning Walczak, Clare Bennet, and Francesco Dazzi

List of Supplementary Materials

Video S4. Living cell imaging of FRET-MSC plated with PHA-aPBMC in the presence of the pan-caspase inhibitor Z-VAD-FMK

Video S5. Living cell imaging of FRET-MSC plated with PHA-aPBMC in the presence of the GrB inhibitor Z-AAD-CMK

Video S6. Living cell imaging of FRET-MSC plated with PHA-aPBMC in the presence of the perforin inhibitor EGTA

Table S1. Clinical features of GvHD patients

Table S2. Primary data

Supplemental Materials and Methods

Mice and disease models

C57BL/6 (H2b) and Balb/C (H2d) mice were purchased from Harlan Laboratories. Mh (C57Bl/6 background, CD8$^+$Tg, H-2b, CD45.2$^+$, H-2Db-restricted) *(55)* mice are transgenic for a T-cell receptor specific for the male antigen UTY presented in the context of H-Db. Mice were bred in-house and maintained at the Biological Service Unit of the Royal Free and University College London Medical School (London, UK) and of Charles River UK Ltd. All mice were used between 6 and 12 weeks of age.

Acute GvHD was induced as previously described *(22)*. Briefly, after lethal irradiation (11 Gy), recipient C57BL/6 male mice were transplanted with 1x10^6 purified CD8$^+$ T cells from female Mh mice, 5x10^6 unfractionated BM and 2x10^6 purified CD4$^+$ T cells from female C57BL/6 wild-type donors. The control group received BM and purified CD4$^+$ cells only. CD4$^+$ and CD8$^+$ T cells were obtained by positive selection using magnetic beads (Miltenyi Biotec Ltd). Live human MSC (1x10^6) were injected i.v. at

day +3, whilst apoMSC ($1x10^6$) were administered i.v. or i.p. at day +1, +3 and +6 from the transplant. Unless otherwise specified, animals were euthanized for analysis at day +7. The infiltration of GvHD effector cells was assessed by flow-cytometry and the percentage was expressed as proportion of cells in the lymphocyte gate, based on the physical characteristics of the cells.

OVA-induced airway inflammation was induced as previously described *(32)*. Briefly, female Balb/C mice (Harlan Laboratories) were injected i.p. with 30 µg of chicken egg albumin (OVA type V) (Sigma-Aldrich Company Ltd) on day 0 and 7. Controls received vehicle (aluminum hydroxide) only. On day 14, 15 and 16 animals were challenged with an aerosolized solution of OVA (3%) for 25 minutes. MSC or ApoMSC were injected 1 hour after the last challenge. After additional 18 hours, mice were terminally anaesthetized with urethane (2 g/kg i.p.) (Sigma-Aldrich Company Ltd), a cannula inserted into the exposed trachea and three 0.5 mL aliquots of sterile saline were injected into the lungs. The total number of cells in the lavage fluid was counted. For differential cell counts, cytospin preparations were stained with Diff Quick (DADE Behring) and cells counted using standard morphological criteria.

In all experiments animals were randomly allocated to control or experimental groups. No blinding approach was adopted. Animal procedures were carried out in compliance with the UK Home Office Animals (Scientific Procedures) Act of 1986.

Cell preparations and media

Cultures were carried out in complete RPMI 1640 medium containing GlutaMAX™, HEPES (25mM), Penicillin 5000 U/ml and Streptomycin 5000 µg/ml (ThermoFisher Scientific), foetal bovine serum 10% (Labtech.com).

Human peripheral blood samples from healthy donors were procured by the National Blood Service (Colindale, UK) as leukocyte cones. Samples from GvHD patients were

collected within 24 hours before MSC injection. Informed consent was obtained in accordance with the local ethics committee requirements. PBMC were isolated by density gradient separation on Histopaque-1077 (Sigma-Aldrich Company Ltd,).

Murine splenocytes were isolated through a cell strainer (BD Falcon), whilst lungs were cut into small pieces and incubated with Collagenase type IV (250 U/ml) (Lorne Laboratories), DNAse I from bovine pancreas (250 U/ml) (Merk Millipore) and foetal bovine serum 6.25% at 37^0 C for 1 hour.

MSC preparations

Clinical grade BM-derived human MSC were generated from BM aspirates collected from the iliac crest of 2 healthy donors. Briefly, 2 ml of BM aspirate were collected in a tube with 100 μl preservative-free heparin. The cells were plated within 24 hours at a density of 10-25 million/636 cm^2 by using alpha modified Eagle's medium (ThermoFisher Scientific), conservative-free heparin (1 UI/ml) (Wockhardt UK Limited) and 5% platelet lysate and then incubated for 3 days at 37 °C and 5% CO_2 ambience. Non-adherent cells were discarded by washing with phosphate buffered saline (ThermoFisher Scientific). When cell confluence of 90-100% was achieved cells were detached with Trypsin-EDTA (0.05% trypsin, 0.5γ mM EDTA•4Na) (ThermoFisher Scientific) and reseeded at a density of 5000 cells/cm^2. MSC were used at passage 2 for all *in vivo* experiments, whilst they were used by passage 8 for the in vitro experiments. In the latter case we did not observe any difference in terms of apoptosis susceptibility between different passages. Released criteria were based on positivity (>80%) for CD105, CD90, CD73, negativity (<2%) for CD3, CD14, CD19, CD31, CD45.

ApoMSC were obtained by plating $5x10^5$ cells per well in a 96 round-bottom well plate in the presence of synthetic human GrB (5 μg/ml) (Enzo Life Sciences) and anti-FAS

human (activating, clone CH11) (10 µg/ml) (Merk Millipore) for 24 hours in complete RPMI. The concentration of GrB and FasL was chosen to produce at least 80% of MSC apoptosis.

Patient details

Between November 2012 and July 2016, 16 patients affected by steroid-resistant GvHD were treated with MSC in the Department of Haematology at Imperial College London, Southampton University Hospital, Bristol Haematology and Oncology Centre and the University Hospital Carl Gustav Carus, Dresden. MSC were administered for compassionate use (according to Regulation (EC) No 1394/2007). Patients had received a myeloablative or reduced-intensity conditioning prior to hematopoietic stem cell transplantation. All patients received GvHD prophylaxis with 3 or 4 doses of methotrexate combined with cyclosporine. T-cell depletion with alemtuzumab or ATG was performed in all adult patients transplanted in the UK centers. Of the 16 patients included in the study, 13 developed GVHD following hematopoietic stem cell transplantation, and the remaining 3 after donor lymphocyte infusions (DLI). 12 patients were affected by acute GvHD, 3 by late onset acute GvHD and 1 by chronic GvHD. The diagnosis of GvHD was made on histological criteria and GvHD staged according to standard criteria *(53, 54)*.

Patients were considered to be steroid-refractory if: (a) those with aGVHD failed to respond to high-dose methylprednisolone after 6 days; (b) the one with cGVHD failed to respond to high-dose steroids after 2-4 weeks, with the addition of Mycophenolate Mofetil (MMF) and cyclosporine at 1 and 4 weeks respectively. Clinical responses to MSC were assessed 1 week after MSC infusion and defined as an improvement of at least 50% in at least one organ affected by GvHD. Patient characteristics are summarized in Table S1.

Imaging of MSC

Luc-MSC were created by transfection with the pGL3-Control vector containing the SV40 promoter for the expression of *Luc+* (Promega) or with pECFP-DEVDR-Venus (Addgene) using electroporation (Gene Pulser Xcell, BioRad). Cells were suspended in a total volume of 250 µl of buffer and electroporated in 0.4 cm gap cuvettes using 10 µg of DNA at 250 volts and 950 F. When pECFP-DEVDR-Venus was used, the donor fluorophore pECFP and the acceptor Venus-YFP were linked through the flexible linker DEVDR which is recognized and cleaved by the active form of caspase 3. In this system caspase 3 activity can be monitored through the analysis of the Förster Resonance Energy Transfer (FRET) between pECFP and Venus-YFP. When caspase 3 is not active, the flexible linker DEVDR remains intact and energy transfer from pECFP is allowed with emission of YFP signal. Conversely, in the presence of caspase 3 activation DEVDR is cleaved, thus energy transfer is lost and the pECFP signal increases.

For confocal imaging, pECFP-DEVDR-Venus transfected MSC were plated in complete RPMI at a concentration of $1x10^5$ cells in a 30 mm x 10 mm dish (Corning) and let adhere overnight. The following day PHA-aPBMC were added at a PBMC:MSC ratio of 40:1. Where indicated, pan caspase inhibitor Z-VAD-FMK (50 µM), perforin inhibitor EGTA (4 mM), GrB inhibitor Z-AAD-CMK (300 µM) were used. Living cell imaging was acquired every 3 minutes for 180 minutes using a Leica TCS-SP5 II Confocal Microscope, with 488 nm and 407 nm lasers. The images were processed and analyzed by using the software "R" and EBImage package.

In vivo imaging was performed injecting i.v. $1x10^6$ luc-MSC into naïve C57BL/6, BM or GvHD mice 3 days after the transplant in the GvHD model. In the airway inflammation model, luc-MSC were infused i.v. in naïve Balb/C or OVA-treated mice 1 hour after the

last OVA challenge. After one additional hour, mice were anesthetized with isoflurane (1.5% isofluorane, 98.5% Oxygen), injected i.p. with 3 mg of VivoGlo Casp 3/7 substrate Z-DEVD Aminoluciferine (Promega,) and imaged using IVIS® Lumina III (PerkinElmer) system for a total time of 5 minutes. Images were analyzed by using the software "R" and EBImage package to obtain mean total luminescence signal (TLS). Confirmation of the presence of transfected MSC was obtained injecting mice with VivoGlo Luciferin (Promega) 30 minutes after the administration of substrate Z-DEVD Aminoluciferine.

Detection of efferocytosis

MSC were first labelled using CellTrace Violet labelling (ThermoFisher Scientific) at a final concentration of 5 µM and then made apoptotic (ApoMSC) as described above, using synthetic human GrB (5 µg/ml) and anti-FAS human (10 µg/ml) for 24 hours. 10×10^6 labelled apoMSC were then injected i.p. or i.v. and mice sacrificed after 2 hours post-injection. Spleen, lungs, peritracheal, paratracheal, pericardial, mesenteric, periportal and celiac lymph nodes were collected and analysed by flow-cytometry. Positivity of CellTrace Violet was assessed as measure of ApoMSC engulfment in $CD11b^+$ and $CD11c^+$ gated subpopulations of phagocytic cells. Cells positive for the CellTrace Violet were then assessed for their expression of IDO.

Pre-activation of human PBMC and murine CD8+ cells

PHA-aPBMC were obtained plating 5×10^6 human PBMC in 24-well plate in the presence of PHA (5 µg/ml) (Sigma-Aldrich Company Ltd) in a final volume of 2 ml of complete RPMI for 72 hours. MLR-aPBMC were obtained using one-way MLR in which PBMC from one donor (stimulators) were irradiated (30 Gy) and co-cultured with the PBMC of an unrelated donor (responder) at a stimulator:responder ratio of 1:1 in

complete medium at a density of 0.75×10^6 cells/cm^2. Cells were then incubated at 37^0 C, 5% CO_2 for 5 days.

NK cells were purified by positively selecting CD56$^+$ cells from healthy donor PBMC (Miltenyi Biotec Ltd) and activated with recombinant human-IL-2 (1000 U/ml) (Peprotec EC Ltd).

NY-ESO1-specific CD8$^+$ T cell clone (Clone 4D8) was kindly supplied by Prof. Vincenzo Cerundolo (Institute of Molecular Medicine, Oxford university, UK). The clone was expanded in complete RPMI 1640 with Sodium Pyruvate (1 mM), 2-Mercaptoethanol (0.05 mM) (ThermoFisher Scientific), recombinant human-IL-2 (400 U/ml) (Peprotec EC Ltd) and PHA (5 µg/ml) (Sigma-Aldrich Company Ltd) *(56)*.

Mh CD8$^+$ were stimulated using the following protocol: 5×10^6 purified CD8$^+$ Mh cells were plated in 24-well plates in the presence of CD3/CD28-coated beads (Dynabeads®) (ThermoFisher Scientific) in a final volume of 2 ml of complete RPMI and incubated for 72 hours.

Immunosuppressive assay

Serial dilutions of human MSC were plated in a flat bottom 96-well plate and let adhere overnight in 100 µl of complete RPMI. Where indicated, MSC cultures were exposed to human Interferon-γ (hIFN-γ) and human TNF-α (hTNF-α), murine IFN-γ (mIFN-γ) and murine TNF- α (mTNF-α) (20 ng/ml each) (all cytokines were from Peprotec EC Ltd), supernatant from PHA-aPBMC or from ConA-aSpl. Both supernatants were obtained from 72-hour stimulation of human PBMC or mSpl with 5µg/ml (PHA) or 3µg/ml (ConA), respectively.

The following day, 5×10^5 Balb/C mSpl were labelled with Carboxyfluorescein Diacetate Succinimidyl Ester dye (ThermoFisher Scientific) and plated with MSC at escalating MSC:mSpl ratios. Culture controls consisted of mSpl plated without MSC in the

presence (positive control) or in the absence (negative control) of ConA (3μg/ml). Proliferation of mSpl was then assessed by flow-cytometry after 72 hours and expressed as the percentage of the proliferation obtained at each MSC:mSpl dilution in comparison with the one obtained in the positive control culture. Results were expressed as percentage of inhibition.

Cytotoxic Assay

$1x10^5$ MSC were plated overnight in a total volume of 500 μl. The day after pre-activated immune cells were plated at different concentrations (2.5 to 40:1 effector:MSC ratios). MSC apoptosis was then tested at different time points using flow-cytometry or confocal microscopy analysis. Eventually, the assay was performed for 4 hours in the vast majority of the cases. At flow-cytometry MSC were identified as CD45$^-$ cells.

Antigen-specific cytotoxic activity of clone 4D8 was tested using T2 cells pulsed with NY-ESO-1 antigen (epitope SLLMWITQC) at a concentration of 0.1 μM for 1 hour.

In the competition assay, T2 (from Hans Stauss, University College London) and K562 cells (from Junia Melo, Imperial College London) were discriminated from effector cells by CellTrace Violet labelling. The tracer concentration was optimized for the T2 (1 μM) and K562 (2.5 μM) cells. Cell lines were tested for mycoplasma contamination before use.

When flow-cytometry was used, the level of apoptosis was assessed using the PE annexin-V apoptosis detection kit (BD Biosciences). Unless specified, apoptotic cells were identified as annexin-V$^+$/7-AAD$^-$ cells.

Inhibitors

Cultures were supplemented with pan-caspase inhibitor Z-VAD-FMK (10 µM in the flow-cytometry experiments or 50 µM in the living cell confocal experiments) (R&D System), perforin inhibitor EGTA (4 mM) (Sigma-Aldrich Company Ltd), GrB inhibitor Z-AAD-CMK (300 µM) (Merk Millipore), neutralizing antibodies against HLA-DR (clone L243) (50 µg/ml), human HLA-A,B,C (clone W6/32) (100 µg/ml) (BD Biosciences), TNF-α antagonist Etanercept (Enbrel®) (10 µg/ml or 100 µg/ml) (Amgen). Each reagent was incubated with MSC 1 hour before the culture with effector killer cells. In all cases, the concentration of the corresponding inhibitor was kept for the duration of the cytotoxic assay.

The neutralizing anti-CD178 (Clone NOK-1) (10 µg/ml or 100 µg/ml) (BD Biosciences), anti-TRAIL (clone 2E2) (10 µg/ml or 100 µg/ml) (Enzo Life Sciences) antibodies, MYR Protein Kinase-Cζ Pseudosubstrate (PKCζ-PS) (10 µM, 25 µM or 75 µM) (ThermoFisher Scientific) and Etanercept (10 µg/ml or 100 µg/ml) were incubated with effector killer cells for 2 hours before the cultures with MSC. In all cases, the concentration of the corresponding inhibitor was kept for the duration of the cytotoxic assay.

Flow-cytometry

The following antibodies specific for murine molecules were used: anti-CD45 (FITC, Clone 30-F11) (eBiosciences Ltd), anti-Vβ8.3 (FITC, Clone 1B3.3), anti-CD8 (APC, Clone 53-6.7), antiCD4 (PE, Clone H129.19), anti-CD19 (APC-H7, Clone 1D3), anti-NK1.1 (PerCP-Cy5.5, Clone PK136) (BD Biosciences), anti-CD11b (PerCP-Cy5.5, clone M1/70), anti-CD11c (APC-Cy7, clone n418), anti-Ido1 (Alexa Fluo647, clone 2e2) (BioLegend). For human specific molecules, the following antibodies were used: anti-CD45 (FITC, clone 2D1), anti-CD8 (APC, Clone SK1), anti-CD4 (PE, Clone SK3),

anti-CD11b (PerCP-Cy5.5, clone M1/70), anti-CD56 (FITC, clone HCD56) (BD Biosciences).

All samples were acquired using BD FACS Canto II using the software FACS Diva and analyzed with Flow-jo software. FRET and Caspase activity (CA$_f$) were assessed by flow-cytometry as previously described *(57)*.

Real Time quantitative PCR

MSC RNA was obtained from TRIzol® (ThermoFisher Scientific) lysates and extracted using RNeasy Mini Kit (Qiagen). Real Time quantitative PCR (qRT-PCR) was performed following TaqMan® RNA-to-CT 1-Step Kit instructions (ThermoFisher Scientific), using 20 ng of RNA template per reaction. Assays were carried out in duplicates on an StepOnePlus RT PCR system thermal cycler (Applied Biosystem) using TaqMan primers (all purchased from ThermoFisher Scientific). The human primers used were the following: IDO2 (Hs01589373_m1), TSG6 (Hs01113602_m1) and PTSG2 (Hs00153133_m1) and HPRT1 (Hs02800695_m1) as housekeeping gene. Data were then analysed using StepOne software version 2.1 and relative quantification obtained with ΔΔCt method, considering untreated MSC as reference.

Figure S1
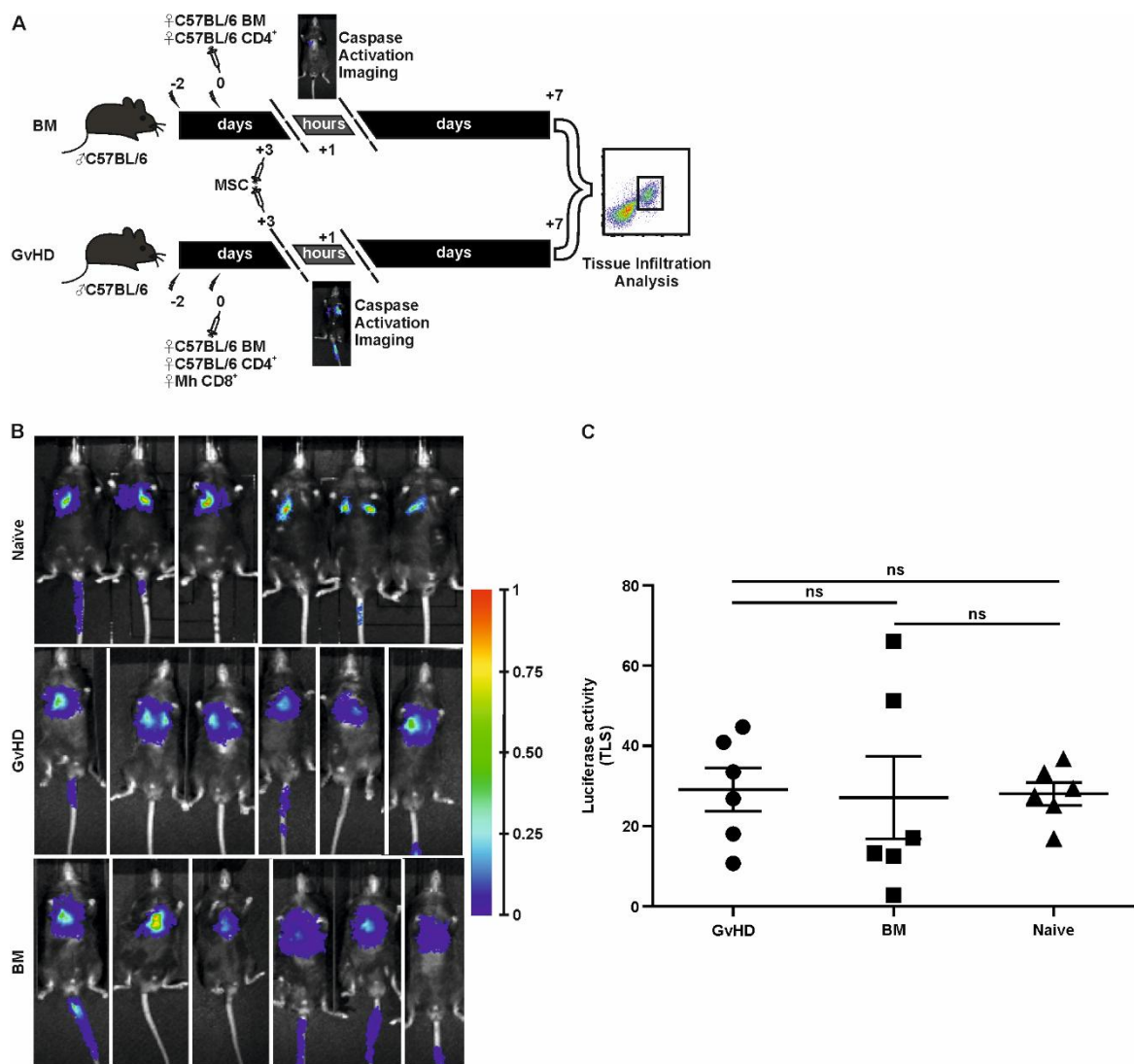
Figure S1. **MSC can be traced in the lungs of mice after infusion**. **A**: Untreated (naïve) or lethally irradiated C57BL/6 male mice were transplanted with bone marrow (BM) and CD4+-purified cells from female syngeneic donors with or without CD8+ cells purified from Mh mice (CD8+V$_\beta$8.3+) (GvHD and BM groups, respectively). At day +3 post-transplant, luc-MSC were infused and mice imaged one hour later for the analysis of caspase 3 activation after i.p. injection of DEVD-aminoluciferin. At day +7 post-transplant, mice were sacrificed and the infiltration of GvHD effector cells (CD8+V$_\beta$8.3+) in lungs and spleen was analyzed by flow-cytometry. **B**: in order to

confirm the presence of luc-MSC in the lungs of all groups of mice infused with MSC, the same mice imaged in Figure 1A were injected with D-Luciferin. White lines separate multiple photographs assembled in the final image. **C**: Total luminescence signal (TLS) was measured from the images of mice in Fig. S1B and shown as mean±SD. Statistics: one-way ANOVA, with Tukey's Multiple Comparison Test. ns: not significant.
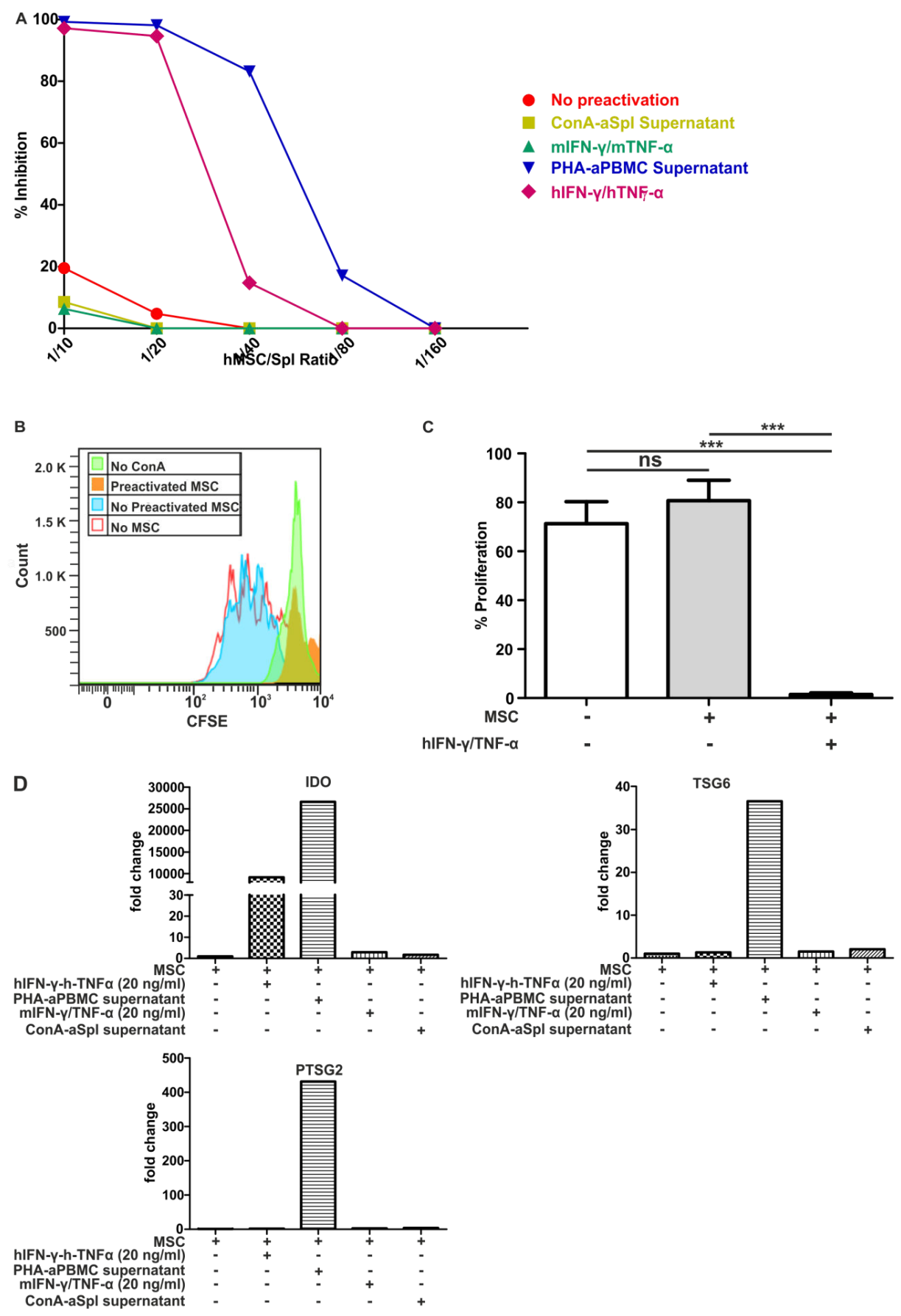
Figure S2

Figure S2. Human MSC immunosuppression is not 'licensed' by murine cytokines. A: human MSC were plated overnight at serial dilutions alone or in the presence of hIFN-γ/hTNF-α (20 ng/ml each) or mIFN-γ/mTNF-α (20 ng/ml each) or supernatant obtained from PHA-aPBMC for 72 hours or mSpl activated with ConA (ConA-aSpl) for 72 hours, as indicated. MSC were then tested for the ability to inhibit the proliferation of ConA-stimulated mSpl labelled with carboxyfluorescein succinimidyl ester dye. Proliferation was determined after 72 hours by flow-cytometry and results expressed as percentage of inhibition in comparison to the positive controls (mSpl stimulated with ConA in the absence of MSC). The curve was obtained plotting the percentage of inhibition against the corresponding MSC:mSpl ratio. **B, C**: human MSC were plated overnight either untreated or exposed to hIFN-γ/hTNF-α (20 ng/ml each) as indicated and then tested for the ability to suppress mSpl proliferation at 1:10 MSC/mSpl ratio. The histogram plot (**B**) is representative of 3 independent experiments, while bars (**C**) represent the mean±SD of 3 independent experiments. Statistics: one-way ANOVA and Tukey's Multiple Comparison test. ***: $p < .001$. ns: not significant. **D**: human MSC were incubated alone or in the presence of hIFN-γ/hTNF-α (20 ng/ml each), mIFN-γ/mTNF-α (20 ng/ml each), supernatants obtained from PHA-aPBMC or ConA-aSpl. After 24 hours, *IDO*, *TSG6* and *PTSG2* expressions were assessed by real time PCR and calculated as relative expression in comparison to untreated MSC. Representative results of three independent experiments are shown.

Figure S3
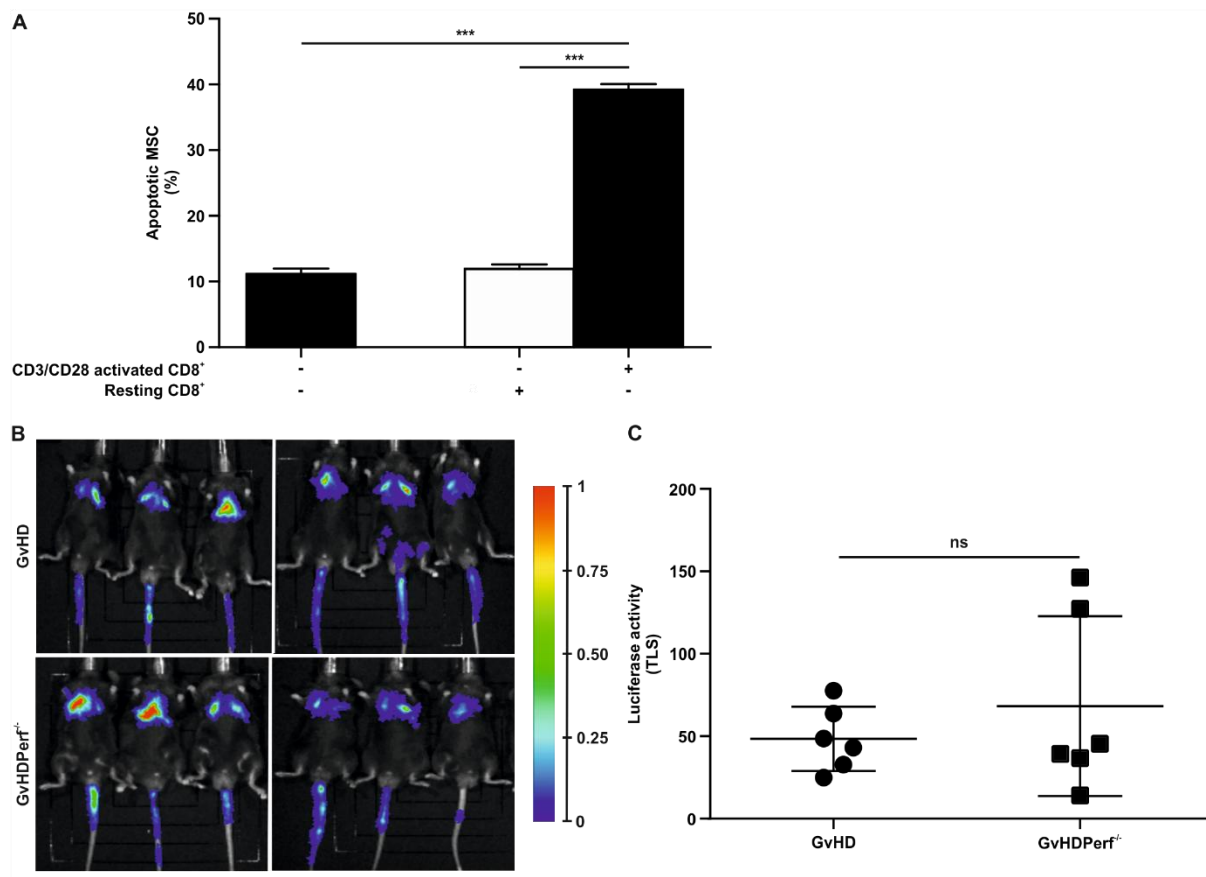
Figure S3. MSC apoptosis is activated by cytotoxic cells in a non-antigen-specific manner. A: CD8^{+} T cells isolated from naïve female Mh mice were stimulated for 3 days with anti-CD3/CD28 beads and cultured with MSC at a 20:1 Mh T-cell:MSC ratio. After 4 hours apoptosis was assessed in MSC by annexin-V/7AAD stainings. Results represent the mean±SD of 3 independent experiments. Statistics: one-way ANOVA, with Tukey's Multiple Comparison Test. ***: p<.001. **B:** in order to confirm the presence of luc-MSC in the lungs of all groups of mice infused with MSC, the same mice imaged in Figure 2C were injected with D-Luciferin. White lines separate multiple photographs assembled in the final image. **C**: Total luminescence signal (TLS) was measured from the images of mice in Fig. S3B and shown as mean±SD. Statistics: unpaired t-test. ns: not significant.

Figure S4
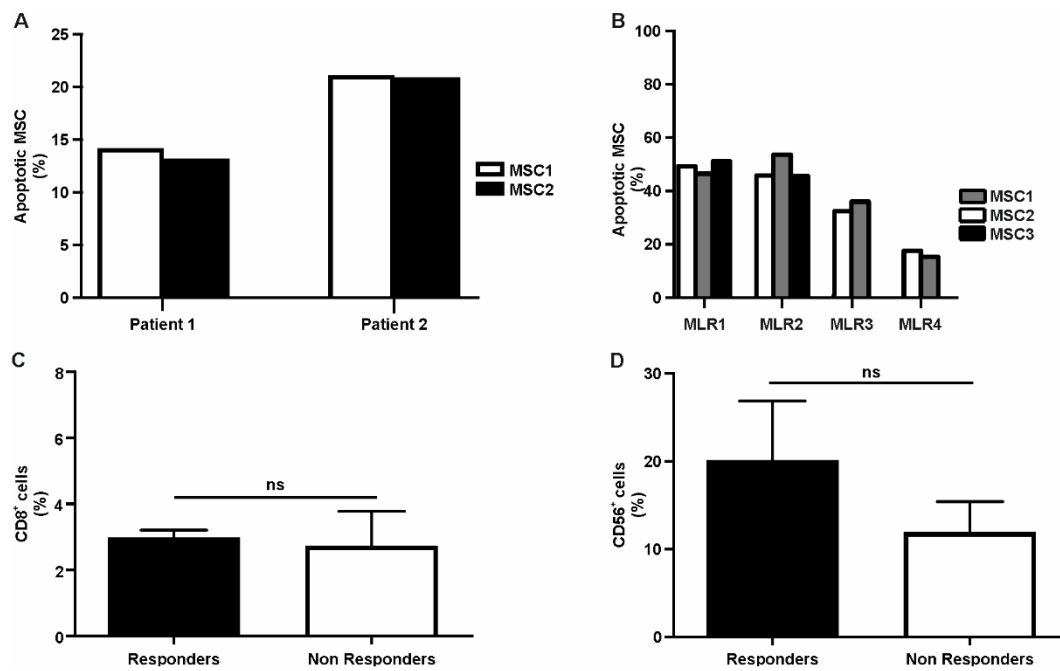
Figure S4. Cytotoxicity against MSC varies amongst PBMC donor but is independent of the percentage of CD8⁺ or CD56⁺ in GvHD patients. A: PBMC obtained from 2 different GvHD patients (Patient 1 and Patient 2) were tested for their cytotoxic activity against MSC from two different donors (MSC1 and MSC2). **B:** apoptosis in MSC obtained from different donors (MSC1, MSC2 and MSC3) after incubation with PBMC from four different MLR responder/stimulator combinations (MLR1, MLR2, MLR3, MLR4). In A and B the level of apoptosis was assessed by flow-cytometry after 4 hours of co-culture. **C, D:** PBMC obtained from 11 GvHD patients (R: 3, NR: 8) were analysed for the percentage of CD8⁺ (**C**) and CD56⁺ (**D**) cells. Statistics: unpaired t-test. ns: not significant.

Figure S5
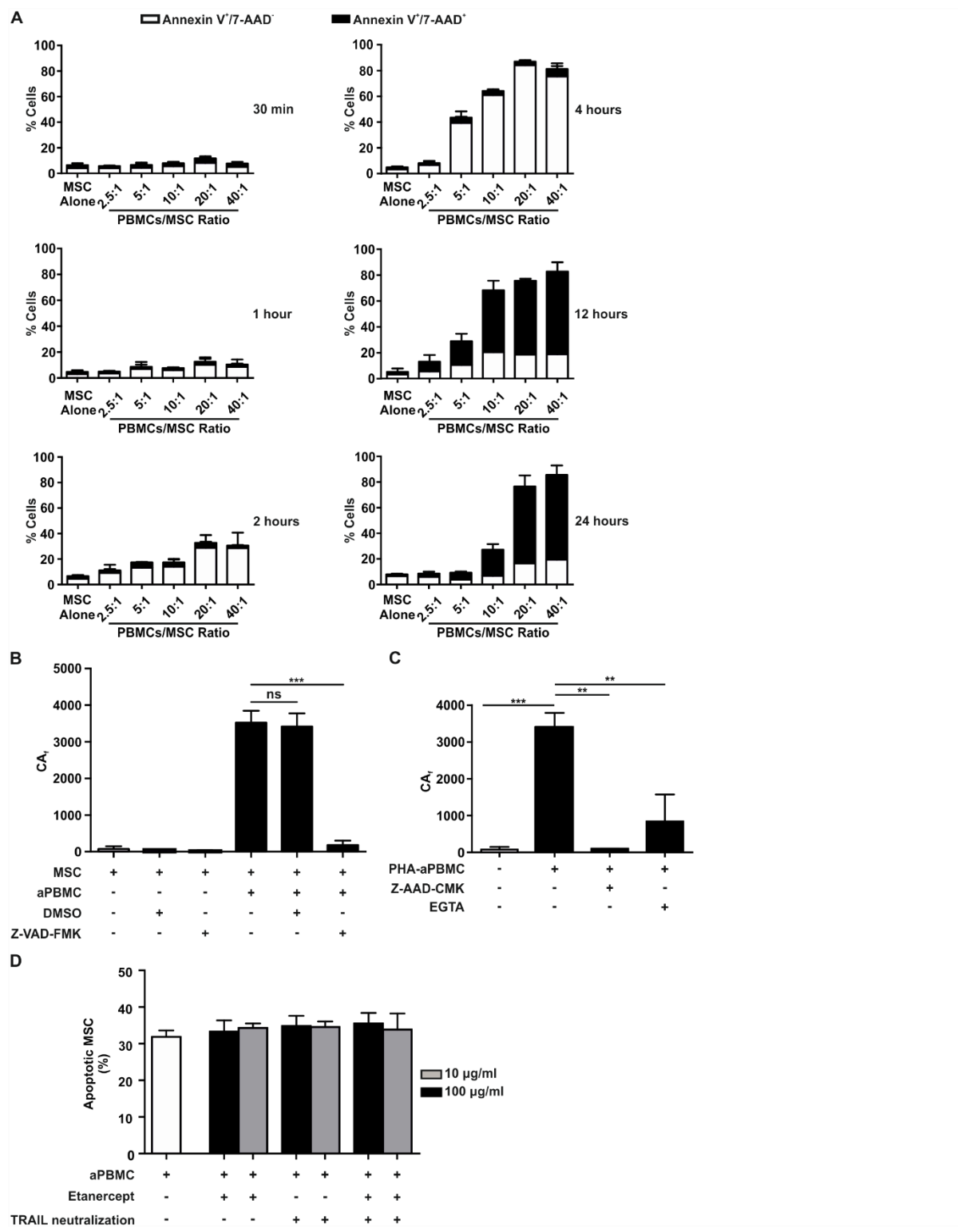
Figure S5. MSC killing is mediated by caspase 3 and effected by GrB and perforin. A: PHA-aPBMC were incubated with MSC at escalating PBMC:MSC ratios. MSC apoptosis was assessed by annexin-V/7-AAD at different time-points by flow-cytometry. Results represent the mean±SD of 3 independent experiments. **B, C**: MSC were transfected with the pECFP-DEVDR-Venus vector (FRET-MSC) and FRET between pECFP and Venus-YFP FRET was studied by flow-cytometry and Caspase activity (CA_f) calculated as described in Materials and Methods. FRET-MSC were cultured alone, with PHA-aPBMC, or PHA-aPBMC in the presence of Z-VAD-FMK (50 µM) (**B**), GrB inhibitor Z-AAD-CMK (300 µM) or the perforin inhibitor EGTA (4 mM) (**C**). Results of 5 (**B**) or 3 (**C**) independent experiments are shown. When PBMC were present, the PBMC:MSC ratio was 40:1. Statistics: one-way ANOVA and Tukey's Multiple Comparison test. **: $p < 01$. ***: $p > .001$. ns: not significant. **D**: MLR-aPBMC were cultivated with MSC (20:1 ratio) and apoptosis evaluated by flow-cytometry 4 hours later. Where indicated, the TNF-α inhibitor Etanercept or the mAb anti-TRAIL were used at 10 µg/ml or 100 µg/ml. Results represents the mean±SD of 3 independent experiments.

Figure S6
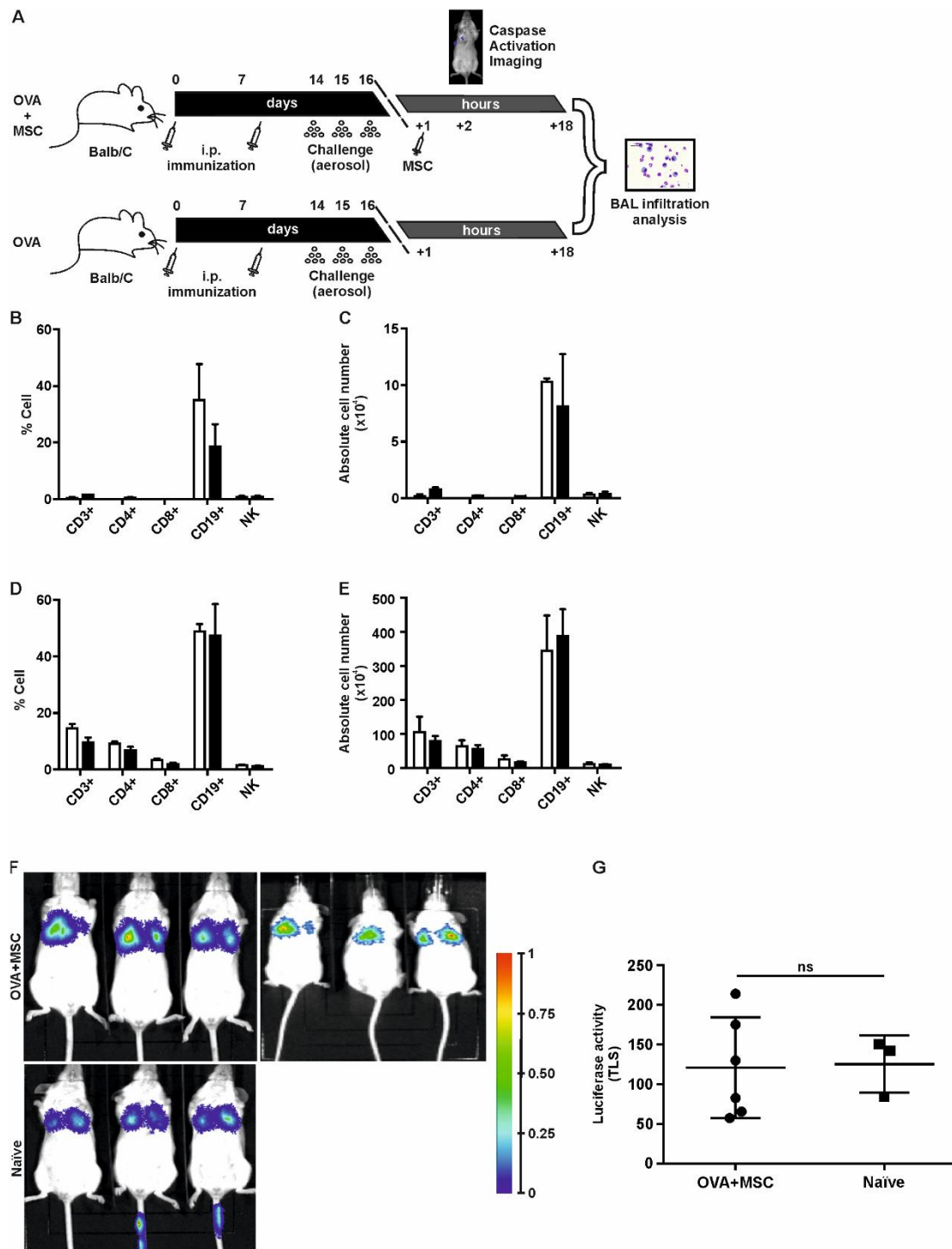
Figure S6. Infused MSC can be imaged in the lungs of mice with Th2-type lung inflammation. A: Balb/C mice were immunized i.p. with OVA at day 0 and 7 and

subsequently challenged with OVA through aerosol at days 14, 15 and 16 (OVA group). Experimental group was treated with MSC one hour after the last challenge (OVA+MSC). When luc-MSC were used, mice were imaged one hour after infusion for the analysis of caspase 3 activation after i.p. injection of DEVD-aminoluciferin. After 18 hours from treatment, eosinophil infiltration in BAL was evaluated. **B-E**: Percentage (**B, D**) and absolute numbers (**C, E**) of different cellular types in the BAL (**B, C**) and lungs (**D, E**) of naïve (with bars) (N=3) and OVA-sensitized (black bars) (N=3) mice. Results represent the mean±SD of 3 independent experiments. In OVA-sensitized mice, the analysis was performed 1 hour after the last aerosol challenge. **F**: in order to confirm the presence of luc-MSC in the lungs of all groups of mice infused with MSC, the same mice imaged in Figure 6A were injected with D-Luciferin. White lines separate multiple photographs assembled in the final image. **G**: Total luminescence signal (TLS) was measured from the images of mice in Fig. S6F and shown as mean±SD. Statistics: unpaired t-test. ns: not significant.

Supplementary Tables.

Table S1. Clinical features of GvHD patients

Diagnosis	Donor type	GvHD	Grade	Organs involved	Concomitant therapy for GvHD	MSC Dose (x10^6/Kg)	Response
DLBCL	SIB	Late onset	3	skin, liver	Steroid, MMF, Infliximab	1.60	NR
CLL	SIB	Late onset	4	gut	Steroid, MMF, Infliximab, Alemtuzumab	2.80	R
HL	VUD	Acute	3	skin, Gut	Steroid	3.00†	NR†
						7.40‡	R‡
CML	VUD	Late onset*	3	Skin, Liver	MMF	3.00	NR
AML	VUD	Chronic*	N/A	Skin	Steroid, CSA	2.70	NR
AML	SIB	Acute	3	Gut	Steroid, CSA	2.10	R
CML	VUD	Acute*	4	Gut	Steroid, CSA	2.90	R
AML	VUD	Acute	4	Skin, gut	Steroid, CSA	3.10	NR
FL	SIB	Acute	4	Skin, gut, Liver	Steroid, CSA, MMF	1.60	R
MM	SIB	Acute	4	Gut	Steroid, Infliximab	2.10	NR
AML	VUD	Acute	4	Gut	Steroids, Budenofalk, CsA	1.28	NR
pre-B ALL	UUD	Acute	4	Skin	Steroids, Topic glucorticoids	1.03	NR
MDS/RAEB-2	VUD	Acute	4	Gut	Steroids, Tacrolimus,MMF, Etanercept, Ruxolitinib, MTX, Alemtuzumab, CsA	1.55	NR
Mixed AML/T-ALL	VUD	Acute	4	Gut	Steroids, CSA	1.33	NR
MM	VUD	Acute	3	Gut	Steroids, CSA	1.01	NR
B-ALL, BCRABL$^+$	SIB	Acute	3	Skin, Liver	Steroids, ECP, CsA	1.11	NR

†: first dose

‡: second dose

*: GvHD post-Donor Lymphocyte Infusion

AML: Acute Myeloid Leukemia; CML: Chronic Myeloid Leukemia; CLL: Chronic Lymphocytic Leukemia; CSA: Cyclosporine; DLBCL: Diffuse Large B-Cell Lymphoma; FL: Follicular Lymphoma; HL: Hodgkin Lymphoma; NR: no response; MM: Multiple Myeloma; MMF: Mycophenolate Mofetil; R: response; SIB: HLA-identical sibling; VUD: Volunteer Unrelated Donor.

Table S2. Primary Data

FIGURE 1						
Panel B **Caspase activity (TLS)**			**Panel C** **GvHD effector cells (spleen)**		**Panel D** **GvHD effector cells (lung)**	
GvHD	**BM Only**	**Naive**	**GvHD**	**GvHD+MSC**	**GvHD**	**GvHD+MSC**
44,1	15,3	0	5,29	7,75	14,4	8,5
29,6	0	1,7	11,7	6,67	18,9	11,3
25,5	13,3	0	16,7	5,07	17	10,5
22,4	0	1,8	14,3	8,91	23,5	13,9
31	2,2	7,7	12,5	5,19	15,8	11,5
6,5	6	0	20,4	13,5	25,1	10,4
			28,8	12,8	18,1	14
			21,6	4,23	17,5	14,5
			11,3	5,54	18,7	10,3
			26,8	6,77	9,25	14,4
			15,1	5,91	20,1	10
			21,4	17,2	29,3	16,5
			16,4	15,2	25,8	11,7
			15,9		31,7	
			29,9		11,2	

FIGURE 2

Panel A CD8⁺Vβ8.3⁺ (%)			Panel D Caspase activity (TLS)		Panel E GvHD effector cells (spleen)		Panel F GvHD effector cells (lung)	
Naive	BM Only	GvHD	BMMhT	BMPerf$^{-/-}$	GvHDPerf$^{-/-}$	GvHDPerf$^{-/-}$+MSC	GvHDPerf$^{-/-}$	GvHDPerf$^{-/-}$+MSC
0,11	1,45	18,92	18,30	8,60	7,92	7,95	22,00	27,00
0,10	0,33	11,76	26,60	4,50	14,80	6,44	24,20	14,50
0,05	0,00	20,66	31,70	4,20	9,25	7,47	21,70	17,70
		14,53	39,10	0,00	11,40	7,38	16,60	13,80
		13,92	26,10	0,00	9,44	7,96	21,10	20,80
		16,45	19,60	10,60	11,70	11,10	18,40	43,80
		18,47	21,10	15,20	27,70	9,75	42,10	41,00
		13,12			38,50	12,80	39,10	31,50
		8,77			23,00	30,00	45,50	50,90
		10,14			4,37	29,50	13,60	56,50
		10,54			4,10	26,90	13,10	55,50
		13,34			7,62	7,47	12,70	20,60
					5,25	14,60	16,00	21,40
					5,93	8,34	16,40	11,90
					5,39	5,89	15,40	14,80
					4,28	8,82	16,80	17,80
						7,00		15,10

FIGURE 3		
Panel B Apoptotic MSC (%)		
HC	NR	R
6,20	0,67	23,00
0,60	4,08	21,10
6,26	13,20	25,30
2,08	3,29	16,50
3,98	11,30	24,50
	10,50	
	1,99	
	0,14	
	0,00	
	3,28	
	8,78	
	11,40	

FIGURE 6

Panel B Caspase Activity (TLS)		Panel C Eosinophils (x10^4/ml)				Panel D Eosinophils (x10^4/ml)		
OVA	Naive	OVA	OVA+MSC	WT+MSC	WT	OVA	OVA+Apo	WT+Apo
0	0	21,92	16,82	0	0	24,745	11,025	0
3,7	0,1	23,4	28,35	0	0	24,605	22,05	0
0	0,2	24,745	20,59	0	0	10,4	3,975	
1,9		24,605	15			31,6	1,35	
0		31,6	37,49			15,08	1,77	
1,1		15,08	12,84			22,25	11,385	
							6,435	

FIGURE 7

Panel A GvHD effector cells (spleen i.p.)		Panel B GvHD effector cells (lung i.p.)		Panel C GvHD effector cells (spleen i.v.)		Panel D GvHD effector cells (lung i.v.)	
GvHD	GvHD+Apo	GvHD	GvHD+Apo	GvHD	GvHD+Apo	GvHD	GvHD+Apo
11,5	4,83	17,1	18,6	21,4	16,7	56,6	53,6
10,3	6,2	18,1	31,9	28,4	16,4	54,6	54,1
11,5	7,15	20,9	11,8	24	16,3	52,7	56,1
6,37	6,54	33,7	9,58	11,5	15	17,1	17,7
17,4	10	27,7	13	10,3	12,7	18,1	18,5
11,7	9,79	13,2	10,3	11,5	7,04	20,9	32,9
9,04	6,12	11,9	10	6,37	8,27	33,7	27,2
11,4	10	13,7	8,28	17,4		27,7	
15,1		14,2		11,7		13,2	
12,9		19,2					

FIGURE 8							
Panel A GvHD effector cells (spleen) Clodronate treatment		Panel B GvHD effector cells (lung) Clodronate treatment		Panel C GvHD effector cells (spleen) 1-DMT treatment		Panel D GvHD effector cells (lung) 1-DMT treatment	
GvHD	GvHD+MSC	GvHD	GvHD+MSC	GvHD	GvHD+MSC	GvHD	GvHD+MSC
20,90	15,80	42,70	42,90	9,11	21,60	15,20	18,50
17,30	16,10	33,60	37,90	24,00	26,20	18,40	7,91
15,80	20,40	36,50	43,60	38,60	20,80	16,40	16,00
16,70	16,60	44,30	24,90	13,40	26,20	12,70	20,70
7,07	10,50	17,10	22,40	35,30	12,50	9,25	13,70
6,80	6,92	20,50	22,70	18,20	25,00	9,44	10,60
8,39	7,41	23,30	22,50	18,40	21,90	11,50	13,70
6,02	20,70	20,90	13,80	19,10	18,00	18,60	9,96
11,30	11,50	10,70	11,10	17,80	19,00	8,73	22,20
6,45	17,70	33,60	15,90		18,50		18,90
16,00		15,60			18,50		9,78
17,40		17,90					

Supplementary Video Legends

Video S1. Living cell imaging of FRET-MSC plated alone. MSC were transfected with the pECFP-DEVDR-Venus vector (FRET-MSC) and caspase 3 activation studied through the analysis of the FRET between pECFP and Venus-YFP. Living cell imaging was acquired every 3 minutes for 180 minutes using a Leica TCS-SP5 II Confocal Microscope, with 488 nm and 407 nm lasers. The images were processed and analyzed by using the software "R" and EBImage package. Red and blue colors correspond to high (high caspase 3 activity) or low (low caspase 3 activity) ECP/FRET ratios, respectively.

Video S2. Living cell imaging of FRET-MSC plated with PHA-aPBMC. As in Video S1 but with FRET-MSC plated with PHA-aPBMC at a PBMC:MSC ratio 40:1.

Video S3. Living cell imaging of FRET-MSC plated with resting PBMC. As in Video S1 but with FRET-MSC plated with resting PBMC at a PBMC:MSC ratio of 40:1.

Video S4. Living cell imaging of FRET-MSC plated with PHA-aPBMC in the presence of the pan-caspase inhibitor Z-VAD-FMK. As in Video S2 but in the presence of the pan-caspase inhibitor Z-VADFMK (50 µM).

Video S5. Living cell imaging of FRET-MSC plated with PHA-aPBMC in the presence of the GrB inhibitor Z-AAD-CMK. As in Video S2 but in the presence of the GrB inhibitor Z-AAD-CMK (300 µM).

Video S6. Living cell imaging of FRET-MSC plated with PHA-aPBMC in the presence of the perforin inhibitor EGTA. As in Video S2 but in the presence of the Perforin inhibitor EGTA (4 mM).